Negatively-charged Amino Acids near and in Transient Receptor Potential (TRP) Domain of TRPM4 Channel Are One Determinant of Its Ca^{2+} Sensitivity

Soichiro Yamaguchi[1, 2], Akira Tanimoto[1], Ken-ichi Otsuguro[1], Hiroshi Hibino[2], and Shigeo Ito[1]

From [1]Laboratory of Pharmacology, Department of Biomedical Sciences, Graduate School of Veterinary Medicine, Hokkaido University, Sapporo, Hokkaido, 060-0818, Japan
[2]Department of Molecular Physiology, Niigata University School of Medicine, Niigata, 951-8510, Japan

To whom correspondence should be addressed: Soichiro Yamaguchi, Laboratory of Pharmacology, Department of Biomedical Sciences, Graduate School of Veterinary Medicine, Hokkaido University, Sapporo, Hokkaido, 060-0818, Japan,
Tel.: (+81) 11-706-5221, Fax: (+81) 11-706-5220,
Email: souya@vetmed.hokudai.ac.jp

Running title: Amino acids in TRP domain of TRPM4 affect Ca^{2+} sensitivity

Keywords: Ion channel; Transient receptor potential channels (TRP channels); Calcium; Manganese; Phosphoinositide; Electrophysiology; Site-directed mutagenesis; Molecular biology; Physiology

---

Background: Transient receptor potential melastatin 4 (TRPM4) channel is activated by intracellular Ca^{2+}.

Results: Cobalt potentiated activation of TRPM4 by Ca^{2+}. Mutations of negatively charged amino acids in TRP domain reduced Ca^{2+} sensitivity.

Conclusion: The acidic amino acids are required for the proper activation of TRPM4 by Ca^{2+}.

Significance: A novel role of TRP domain in TRPM4 was suggested.

ABSTRACT

Transient Receptor Potential (TRP) channel Melastatin subfamily member 4 (TRPM4) is a broadly expressed nonselective monovalent cation channel. TRPM4 is activated by membrane depolarization and intracellular Ca^{2+}, which is essential for the activation. The Ca^{2+} sensitivity is known to be regulated by calmodulin and membrane phosphoinositides, such as PI(4,5)P_2. Although these regulators must play important roles in controlling TRPM4 activity, mutation analyses of the calmodulin binding sites have suggested that Ca^{2+} binds to TRPM4 directly. However, the intrinsic binding sites in TRPM4 remain to be elucidated. Here, by using patch-clamp and molecular biological techniques, we show that

there are at least two functionally different divalent cation binding sites and the negatively charged amino acids near and in the TRP domain in C-terminal tail of TRPM4 (D1049 and E1062 of rat TRPM4) are required for maintaining the normal Ca^{2+} sensitivity of one of the binding sites. Applications of Co^{2+}, Mn^{2+}, or Ni^{2+} to the cytosolic side potentiated TRPM4 currents, increased the Ca^{2+} sensitivity, but were unable to evoke TRPM4 currents without Ca^{2+}. Mutations of the acidic amino acids near and in the TRP domain, which are conserved in TRPM2, TRPM5, and TRPM8, deteriorated the Ca^{2+} sensitivity in the presence of Co^{2+} or $PI(4,5)P_2$ but hardly affected the sensitivity to Co^{2+} and $PI(4,5)P_2$. These results suggest a novel role of the TRP domain in TRPM4 as a site responsible for maintaining the normal Ca^{2+} sensitivity. These findings provide more insights into the molecular mechanisms of the regulation of TRPM4 by Ca^{2+}.

Transient Receptor Potential Channel Melastatin (TRPM), a subfamily of the TRP ion channel, consists of eight channels, TRPM1 to TRPM8. Among the TRPM channels, TRPM4, as well as TRPM5, forms a Ca^{2+}-activated nonselective monovalent cation channel, which does not conduct divalent cations such as Ca^{2+} (1) although other TRPM channels permeate them (2). TRPM4 does not differentiate Na^+ and K^+ (3,4), and its opening affects cell functions through membrane depolarization. Unlike TRPM5, TRPM4 has a relatively broad tissue expression pattern (4). In those tissues, TRPM4 has been implicated in several physiological functions, for example, immune response (5-7) and constriction of cerebral arteries (8,9). Additionally, its mutations in the TRPM4 gene have been associated with cardiac conduction dysfunction in human patients (4,10-12). Furthermore, it has been shown that TRPM4 mediates axonal and neuronal degeneration in experimental autoimmune encephalomyelitis and multiple sclerosis (13).

TRPM4 channel activity is increased by membrane depolarization, but it absolutely requires intracellular Ca^{2+} (14). Thus, the most important regulator of TRPM4 activity is the intracellular Ca^{2+}. However, the activation mechanisms of TRPM4 by Ca^{2+} have not been completely clarified. Calmodulin is thought to play an important role in the activation of TRPM4 by Ca^{2+} through its binding to the C-terminal tail of TRPM4 because it has been reported that deletion mutants of calmodulin binding sites showed strongly impaired current activation by reducing Ca^{2+} sensitivity (14). For example, although wild-type TRPM4 has shown large currents in the presence of 100 μM Ca^{2+}, the mutants have shown negligible currents under the same conditions (14). However, the mutants were still able to be activated by very high concentrations (e.g. 1 mM) of Ca^{2+} and positive voltages (14). Furthermore, TRPM5, which shows the highest homology to TRPM4 (4), has been suggested to be activated by Ca^{2+} directly rather than through calmodulin because calmodulin modulators did not affect TRPM5 (15). These

findings imply that there are unidentified intrinsic Ca^{2+} binding sites in TRPM4 as mentioned elsewhere (4,14). Moreover, a membrane phospholipid, Phosphatidylinositol-4,5-bisphosphate ($PI(4,5)P_2$, PIP_2), has been shown to restore the Ca^{2+} sensitivity of TRPM4 after desensitization (16,17). For example, the EC_{50} for Ca^{2+} after desensitization was reported to be 520 μM, and that after application of PIP_2 was 120 μM (16). Positively charged amino acids in a C-terminal pleckstrin homology (PH) domain were identified as important determinants of PIP_2 action (17). However, the mechanism of how PIP_2 increases the Ca^{2+} sensitivity of TRPM4 has not been revealed.

The C-terminal cytosolic tail of TRPM4, which is important for the regulation of its activity, contains the TRP domain and TRP box. The TRP domain refers to a homologous block of about 25 residues immediately C-terminal to S6 that is loosely conserved in almost all TRP mammalian subfamilies (18). The TRP domain encompasses a highly conserved 6-amino acid TRP box (18). The TRP domain of TRPM8, TRPM5, and TRPV5 has been suggested to serve as a PIP_2-interacting site (19). However, it has been shown that the TRP box and TRP domain of TRPM4 are not the main determinants of PIP_2 action (17). Therefore, the functional role of the TRP domain and TRP box in TRPM4 remains elusive.

Ca^{2+} binding sites of Ca^{2+}-regulated proteins exhibit diverse divalent cation selectivities. Thus, the divalent cation selectivities of binding sites have been used as a powerful tool for distinguishing properties of different Ca^{2+} binding sites in conjunction with the molecular biological approaches. For example, it has been shown that the large-conductance Ca^{2+}-activated K^+ channel, BK channel, has three divalent cation binding sites, the so-called Ca^{2+}-bowl, RCK1 domain, and E399-related low-affinity sites, of which divalent cation selectivities are different (20,21). On the basis of such an idea, it has been shown that Sr^{2+} and Ba^{2+} do not substitute for Ca^{2+} in TRPM4 activation (22). However, not much has been done to reveal the overall mechanisms of the activation of TRPM4 by Ca^{2+}, such as the number of binding sites in TRPM4 and their roles in the activation by Ca^{2+}.

The objective of this paper is to obtain further understanding of the mechanisms underlying the activation of TRPM4 by intracellular Ca^{2+}. In order to reveal the properties of divalent cation binding sites of TRPM4, we firstly examined the effects of larger variety of divalent cations applied to the cytosolic side of the channel. Secondly, we explored the amino acid residues responsible for the activation by Ca^{2+} using single amino acid mutagenesis approaches. Among several mutants of the amino acid residues in the cytosolic C-terminal tail of TRPM4, we found two negatively-charged amino acids near and in the TRP domain of TRPM4 to be important determinants of Ca^{2+} sensitivity.

EXPERIMENTAL PROCEDURES

Animal Ethics Approval − All animal experiments

were performed in accordance with guidelines from and protocols approved by the Institutional Animal Care and Use Committee (IACUC), Graduate School of Veterinary Medicine, Hokkaido University and the Committee on Animal Experimentation, Niigata University School of Medicine.

Molecular cloning and Site-directed Mutagenesis − TRPM4b, the long form of TRPM4, forms a functional channel and considered to be the significant variant (3). Therefore, we refer to TRPM4b as TRPM4 in this paper. Rat TRPM4 was cloned from mRNA of the stria vascularis in the cochlea because Ca^{2+}-activated nonselective currents were recorded from the apical membrane of marginal cells in freshly isolated stria vascularis using inside-out mode of patch clamp technique (data not shown) as similarly reported from those of guinea pig (23) and gerbil (24). Additionally, the expression of TRPM4 in the marginal cells has been confirmed by immunohistochemistry more recently (25). RNA was extracted from stria vascularis in the cochleae of BN/SsNSlc male rats (5-6 weeks old) using NucleoSpin RNA XS (Takara Bio, Otsu, Japan). cDNA was synthesized using PrimeScript II Reverse Transcriptase (Takara Bio). The full length of the open reading frame of TRPM4 cDNA was amplified as two overlapped N-terminal and C-terminal fragments by PCR using a high fidelity polymerase (PrimeSTAR GXL, Takara Bio) and the following primers: 5' GGC GGC TGA GAG AAA TAC ACG GAG C 3' (N-terminal Forward) and 5' GTC ACT CCA GGG GGC TTG TTC AAA G 3' (N-terminal Reverse), 5' AAC TTT TCC GTG GGG ACA TCC AGT G 3' (C-terminal Forward) and 5' CAT GGG GTC TAC GGT GAG GAC AAG G 3' (C-terminal Reverse), respectively. The primers were designed based on the reported sequence of rat TRPM4 cDNA (Genbank accession #NM_001136229.1). The two fragments of TRPM4 were cloned in TA-vector (Takara Bio) and sequenced. The nucleic acid and amino acid sequences of the cloned rat TRPM4 were identical to those recorded in database (#NM_001136229.1 and #NP_001129701.1, respectively (26)). The N-terminal and C-terminal fragments, which contained no PCR errors, were subcloned and combined in a bicistronic expression vector pIRES2-EGFP (Takara Bio). Site-directed mutagenesis of TRPM4 cDNA in pIRES2-EGFP was accomplished using the PrimeSTAR Mutagenesis Basal kit (Takara Bio). Mutations were verified by DNA sequencing.

Cell culture and transfection − HEK 293T cells were cultured in DMEM (Dulbecco's modified Eagle's medium; Sigma-aldrich, St. Louis, MO) supplemented with 10% FBS (Moregate Biotech, Bulimba, Australia, or Thermo Fisher Scientific, Waltham, MA. Their local distributors were Hana-nesco Bio, Tokyo, Japan and Thermo Fisher Scientific K.K., Yokohama, Japan, respectively.) and penicillin/streptomycin (1000 U/ml and 1000 μg/ml, respectively, Thermo Fisher Scientific) at 37 °C in a 5% CO_2 incubator. Cells were

transiently transfected with plasmids using TransIT-293 Transfection Reagent (Takara Bio). The cells were plated on coverslips the following day. Patch-clamp recordings were made two days after transfection from EGFP positive cells, which were identified with an inverted microscope (Diaphot 300, Nikon, Tokyo, Japan) equipped with a super high-pressure mercury lamp light source (C-SHG, Nikon) for excitation of green fluorescence from EGFP.

Electrophysiology − HEK 293T cells on coverslips were transferred to a bath mounted on the stage of the inverted microscope and superfused with a standard NaCl rich solution containing 145 mM NaCl, 5 mM KCl, 1 mM $MgCl_2$, 1 mM $CaCl_2$, 10 mM D-glucose, and 10 mM HEPES (pH = 7.4 with NaOH). The pipette solution contained 145 mM NaCl, 1 mM $MgCl_2$, 1 mM $CaCl_2$, and 10 mM HEPES (pH = 7.4). Before patch excision, the bath solution was changed to mainly a solution containing 145 mM NaCl, 10 mM HEPES (pH = 7.4), and 1 mM $CaCl_2$. In many cases, a divalent cation-free solution contained 5 mM EGTA to chelate divalent cations but in some experiments, a nominally divalent cation-free solution was also used, which was made simply without adding divalent cations. Dichloride salts of divalent cation were used. The concentration of free Ca^{2+} in solutions less than 10 μM was adjusted by adding an appropriate amount of $CaCl_2$, calculated using a software webmaxc (http://www.stanford.edu/~cpatton/webmaxcS.htm), to solutions containing 5 mM EGTA. In some experiments, o-phenylenedioxydiacetic acid (o-PDDA, Sigma-aldrich) was used as a divalent cation chelator and free divalent cation concentrations were calculated with the stability constants reported elsewhere (27). Na-fluoride (NaF, 145 mM) was also used as a Ca^{2+}-chelator (21,28). Osmolality of solutions were measured using Vapro Vapor Pressure 5600 (Wescor Inc, Logan, UT, USA). The osmolality of most solutions were near physiological range e.g. that of the pipette solution was 283 ±2 mOsm/kg, that of nominal Ca^{2+}-free solution was 276 ±1 mOsm/kg, and that of the solution containing 10 mM $CaCl_2$ was 301 ±0 mOsm/kg. However, the osmolality of the solution containing 30 mM $CaCl_2$ was 352 ±1 mOsm/kg. The results of the present study might be partially affected by the change in osmolality as a background effect. The speed of perfusion was about 1.5 ml/min. The bath solution around a patch membrane was cleared within 10 sec in most cases or within 15 sec at the latest.

Axopatch 200B patch-clamp amplifier, digidata 1322A, and the pCLAMP8 software (Axon Instruments, Union City, CA) were used to perform voltage clamp, data storage, and analysis. A reference Ag–AgCl electrode was connected into the bathing solution via an agar bridge filled with the aforementioned standard NaCl-rich bath solution. Patch electrodes had a resistance between 3 and 5 megaohms. The currents were filtered at 1 kHz with an internal four-pole Bessel

filter, and sampled at 5 kHz. Current–voltage (*I-V*) relations for the currents were studied using voltage ramps. The membrane potential held at −60 mV, and the command voltage was varied from −100 to +100 mV over a duration of 400 ms following a prepulse of −100 mV for 50 ms every 5 s. Because TRPM4 is activated by membrane depolarization, we analyzed the current amplitudes at −100 mV and +100 mV as the least and the most activated current among the currents evoked by the applied pulse, respectively. Furthermore, because the current amplitudes at −100 mV in some mutants were negligible, the current amplitudes at +100 mV were used for the analysis of dose-response. All experiments were performed at room temperature.

Data analysis − Dose-response curves were fits of the averages with the Hill equation:

$$I = I_{max} \times \frac{C^n}{{EC_{50}}^n \times C^n}$$

where I_{max} is the maximum currents, C is the concentration of substance being tested, EC_{50} is the concentration for half-maximal effect, n is the Hill coefficient. The relationship between EC_{50} for Ca^{2+} and the concentration of Co^{2+} was analyzed with the pseudo Hill equation:

$$y = y_{max} + (y_{min} - y_{max}) \times \frac{C^n}{{EC_{50}}^n \times C^n}$$

where y_{max} is the EC_{50} for Ca^{2+} in the absence of Co^{2+} and y_{min} is the minimal EC_{50} for Ca^{2+} among those estimated in the presence of Co^{2+}, C is the concentration of Co^{2+}, EC_{50} is the concentration of Co^{2+} for half-maximal effect, n is the pseudo Hill coefficient. Chord conductance-voltage curves were fitted with the Bolzmann equation:

$$G = G_{max} \times (1 - \frac{1 - f}{1 + e^{(V_m - V_{1/2})/dx}})$$

where G_{max} is fixed to the normalized conductance at +100 mV, V_m is the membrane potential, $V_{1/2}$ is the membrane potential at which the conductance is half of G_{max}, dx is the slope factor, and f is the voltage-independent conductance fraction. All curves were obtained by fitting the data averages.

The results are reported as means ±S.E. of independent experiments (n), where n refers to the number of cells patched. Statistical significance was evaluated using Student's two-tailed paired or unpaired t test or Dunnett's test as appropriate. A value of $P < 0.05$ was considered significant.

RESULTS

Effects of divalent cations on TRPM4 currents

Rat TRPM4 showed outward rectifying currents after the inside-out patch excision in the presence of 1 mM Ca^{2+} in the perfusate, and the currents were decreased probably mainly by a decline in the sensitivity of the channels to Ca^{2+} (14), which is most likely due to the loss of PIP_2 as in well-studied human TRPM4 (16,17,29) (Fig. 1A). The TRPM4 currents were abolished when the Ca^{2+} in the bath solution, which faces the cytoplasmic side of the ion channel, was removed (Fig. 1A). Although it has been reported that HEK 293 cells express endogenous TRPM4 (1,30), no Ca^{2+}-activated currents were recorded from our mock transfected HEK 293T cells, and on the

contrary the background outward currents were increased when Ca^{2+} in the solution was removed (in the presence of 1 mM Ca^{2+}: 9.2 ±2.3 pA; in the absence of Ca^{2+}: 11.9 ±2.2 pA at +100 mV, n = 8, typical *I-V* curves are shown in the inset to Fig. 1B). The discrepancy might be due to differences in cell clones or in culture conditions such as serum. The Ca^{2+}-inhibitable currents may be endogenous TRPM7 currents (31), which are inhibited by millimolar concentrations of intracellular Ca^{2+} as well as Mg^{2+} (32,33). At least as macroscopic currents the background endogenous TRPM4 currents had little effect on the analysis of heterologously expressed TRPM4 currents in our system.

First of all, we examined effects of divalent cations on the desensitized TRPM4 currents. After the current amplitudes became almost stable in the presence of 1 mM Ca^{2+}, 1 mM of several divalent cations (Ca^{2+}, Co^{2+}, Mn^{2+}, Ni^{2+}, Mg^{2+}, Ba^{2+}, Sr^{2+}, Cd^{2+}, and Zn^{2+}) were co-applied with 1 mM Ca^{2+} to the intracellular perfusate. When the current amplitude was judged to have reached a steady state, the relation of the current amplitude to the previous data value at +100 mV was 98.8 ±0.6% (n = 80) and that at −100 mV was 100.8 ±2.0% (n = 80). However, the current amplitudes were gradually slightly decreased throughout the measurements in many cases. Therefore, in order to eliminate the influence of variations in current amplitudes among the time of measurement and among the patch membranes, the current amplitudes were normalized to those recorded in the presence of 1 mM Ca^{2+} right before exposure to the other divalent cations. Co^{2+}, Mn^{2+}, and Ni^{2+} potentiated TRPM4 currents (Fig. 1A-C), made the *I-V* curve of TRPM4 currents linear (Fig. 1B), and increased the voltage-independent conductance fraction (Fig. 1D). The currents potentiated by Co^{2+} were inhibited by a TRPM4 inhibitor, fulfenamic acid (34) (Sigma-aldrich, 100 μM, Fig. 2). However, 100 μM FA did not completely inhibit the Co^{2+}-potentiated TRPM4 currents. The slight reduction of the inhibition by FA might be due to an allosteric change of TRPM4 structure by the binding of Co^{2+}, which may also cause the increase in the current amplitudes. In excised patches from mock transfected cells, 1 mM Co^{2+} or even 10 mM Mn^{2+}, co-applied with 1 mM Ca^{2+}, did not evoke any currents in comparison with the Ca^{2+}-free condition (inset to Fig. 1B, n = 6). Mg^{2+} had no effect on TRPM4 currents (Fig. 3). Cd^{2+} and Zn^{2+} abolished TRPM4 currents and chelation with EDTA was required to reactivate TRPM4 currents fully with Ca^{2+} (Fig. 3). Effects of Ba^{2+} and Sr^{2+} were not consistent; they blocked TRPM4 currents 4 out of 7 (Ba^{2+}) or 4 out of 8 (Sr^{2+}) membrane-patch recordings, respectively, but showed no effect on the currents in other cases (Fig. 3). The results, which indicate that Ba^{2+} and Sr^{2+} at least do not activate TRPM4, are partially consistent with the report that Ba^{2+} and Sr^{2+} cannot substitute for Ca^{2+} in TRPM4 channel activation (22).

Existence of two functionally different divalent cation binding sites

Preliminary experiments using nominally Ca^{2+}-free solution showed that effects of Co^{2+}, Mn^{2+}, and Ni^{2+} without Ca^{2+} were none or weaker than those in the presence of 1 mM Ca^{2+}. Therefore, we assumed the effects of Co^{2+}, Mn^{2+}, and Ni^{2+} were dependent on Ca^{2+}. To test the effects of Co^{2+}, Mn^{2+}, and Ni^{2+} in the absence of Ca^{2+}, we used fluoride as a Ca^{2+} chelator because common divalent cation chelators, such as EGTA and EDTA, bind to Co^{2+}, Mn^{2+}, and Ni^{2+} with a higher affinity than Ca^{2+}. In solutions containing 145 mM NaF, because of the lack of solubility of CaF_2, the fluoride ion removes free Ca^{2+} from such solutions so that the effective free Ca^{2+} concentrations can be considered less than 20 nM (21,28). In contrast, 1 mM Mn^{2+}, Co^{2+}, and Ni^{2+} remain soluble (21,28). Perfusion with the Ca^{2+}-free solution containing fluoride eliminated the TRPM4 currents at the same level as that containing EGTA (Fig. 4A). One mM Mn^{2+}, Co^{2+}, and Ni^{2+} did not evoke any currents in the Ca^{2+}-free solution containing fluoride (Fig. 4A).

We cannot completely exclude the possibility that the fluoride itself inhibited TRPM4 and so that TRPM4 currents were not evoked by Mn^{2+}, Co^{2+}, and Ni^{2+} in the presence of fluoride. Therefore, we also used another divalent cation chelator, *o*-phenylenedioxydiacetic acid (o-PDDA, the same with 1,2-Phenylenedioxydiacetic acid, Sigma-aldrich). The stability constants of o-PDDA for Ca^{2+} and Co^{2+} are 3.1 and 1.1, respectively (27), which means that o-PDDA binds to Ca^{2+} with a higher affinity than Co^{2+}. On the other hand, the stability constants of Mn^{2+} and Ni^{2+} are 2.8 and 1.6, respectively (27). That means Co^{2+} has the least inhibitory effect on the Ca^{2+}-chelating action of o-PDDA among these three divalent cations. Therefore, we used Co^{2+} in this experiment. Even when the free Ca^{2+} concentration was controlled by the chelation with 6 mM o-PDDA, 1 mM Ca^{2+} evoked TRPM4 currents, and 1 mM Co^{2+} potentiated the currents in the presence of Ca^{2+} but did not evoke any currents in the absence of Ca^{2+} (Fig. 4B).

These results indicate not only that the effects of Co^{2+}, Mn^{2+}, and Ni^{2+} were dependent on Ca^{2+} but also there are at least two functionally different divalent cation binding sites in TRPM4 and/or its associated proteins. One is a relatively Ca^{2+}-specific binding site, which has a negligible affinity for Co^{2+}, Mn^{2+}, and Ni^{2+}, and the other is a biding site for Co^{2+}, Mn^{2+}, and Ni^{2+} (Fig. 4C). The Ca^{2+}-dependence of the effects of Co^{2+}, Mn^{2+}, and Ni^{2+} implies that only the binding of divalent cations to the 2nd binding site do not open the TRPM4 channel and the binding of Ca^{2+} to the 1st binding site is probably necessary to open the TRPM4 channel.

Mutations of negatively-charged amino acids near and in TRP domain reduce Ca^{2+}sensitivity and voltage dependence

To explore the divalent cation binding sites of TRPM4, we performed analysis of point mutations causing a single amino acid substitution in the cytosolic C-terminal region. Among the mutations of several negatively-charged acidic amino acids, we found mutations of two amino

acids near and in the TRP domain that altered the function of the TRPM4 channel. One is the aspartate just before the TRP domain (1049th aspartate: D1049 of rat TRPM4) and the other is the glutamate in the TRP domain (1062nd glutamate: E1062 of rat TRPM4) (Fig. 5A). These amino acids are conserved across species (*Mus muscles*: Genbank accession # NP_780339, *Homo sapiens*: #NP_001182156, *Pan troglodytes*: # JAA33534, and *Danio rerio*: # NP_001275744). Intriguingly, the amino acids are also conserved in the other (directly or indirectly) Ca^{2+}-sensitive TRPM channels, TRPM5 (3), TRPM2 (35), and TRPM8 (36) (Fig. 5A). The other acidic amino acids which we tested were E1112, D1133, D1136, D1138, E1140, D1150, E1161, D1163, E1170, and E1172. The mutants of these amino acids did not show clear differences from wild-type (WT) TRPM4.

After desensitization, WT TRPM4 currents were evoked by 0.3 mM Ca^{2+} and saturated by 3 mM Ca^{2+} at +100 mV (Fig. 5B and C). Analyses of the currents at +100 mV showed that the mutations of D1049 to asparagine (D1049N) and to alanine (D1049A) only slightly, and those of E1062 to glutamine (E1062Q) and to alanine (E1062A) comparatively largely reduced Ca^{2+} sensitivity, respectively (Fig. 5B and C). The values of normalized current amplitudes of the mutants except D1049A were significantly different from those of WT at 1 and/or 3 mM Ca^{2+}. The EC_{50} values for Ca^{2+} and Hill coefficients were summarized in Table 1. The maximal current amplitudes of WT and mutants evoked by Ca^{2+} were summarized in Table 2. The surface expression level, which is assumed from the current amplitudes, may be also affected by the mutations but it is not correlated to the Ca^{2+} sensitivity. All the mutants maintained the reactivity to Co^{2+}, Mn^{2+}, and Ni^{2+} since their currents were potentiated by application of 1 mM Co^{2+} (Fig. 5B), Mn^{2+}, or Ni^{2+} (Fig. 6). Double mutants of D1049N and E1062Q were active but their steady state currents were too small to analyze (data not shown).

The mutations of D1049 and E1062, except E1062A, changed also the voltage dependence. D1049N, D1049A, and E1062Q mutants lost the inward currents evoked by Ca^{2+} at −100 mV (Fig. 5B). As shown in Figure 7A, the *I-V* relationships of D1049N, D1049A, and E1062Q mutants had a strongly outward rectification in the presence of 3 mM Ca^{2+}. Curiously, the *I-V* curve of E1062A resembled with that of WT TRPM4 (Fig. 7A). The ratios of currents at −100 mV to those at +100 mV of D1049N, D1049A, and E1062Q mutants were significantly smaller than that of WT TRPM4 (Fig. 7B). For each construct, *G-V* curves at different [Ca^{2+}] were obtained from currents evoked by ramp pulses and fit with Boltzmann functions (Fig. 7C). A raise in [Ca^{2+}] increased the voltage-insensitive conductance fraction of WT TRPM4 and the E1062A mutant but scarcely affected that of D1049N, D1049A, and E1062Q mutants (Fig. 7C). These results indicate that D1049 and E1062 are necessary for the normal Ca^{2+} sensitivity and voltage dependence of TRPM4. Moreover, the mechanisms controlling

these two properties must be related but not completely coupled with each other since the E1062A mutation affected only one of them.

Mutations of D1049 and E1062 decrease the Ca^{2+} sensitivity of the apparently Ca^{2+}-specific binding site

Which divalent cation binding sites, suggested by their different affinities for divalent cations, are affected by the mutations of D1049 and E1062? To answer the question, we evaluated the affinities of the 1st and the 2nd binding sites. First, we found that Co^{2+} increased Ca^{2+} sensitivity of WT TRPM4. As shown in Fig. 8A, in the presence of 1 mM Co^{2+}, Mn^{2+}, or Ni^{2+}, TRPM4 currents were substantially evoked by 0.1 mM Ca^{2+}. The Ca^{2+} dose-response curves for TRPM4 currents were shifted to the left by the co-application of Co^{2+} (Fig. 8B). EC_{50} for Ca^{2+} was decreased by the co-application of Co^{2+} (e.g. 0.96 mM without Co^{2+}, 107 μM with 1 mM Co^{2+}). These results suggest that the binding of Co^{2+} to the 2nd binding site increased the affinity for Ca^{2+} of the 1st binding site. The EC_{50} for Co^{2+} was 57.5 μM, which was calculated from the shift of EC_{50} for Ca^{2+} and is deemed to reflect the affinity of the 2nd binding site.

Ca^{2+} sensitivities of D1049N and E1062Q mutants were likewise increased by co-application of Co^{2+} (Fig. 8C and 8D). The EC_{50} for Ca^{2+} of D1049N and E1062Q mutant currents were decreased by the co-application of Co^{2+} as in WT TRPM4 although the absolute values of EC_{50} for Ca^{2+} were different from that of WT TRPM4 (Fig. 8E). The EC_{50} for Ca^{2+} normalized in the absence of Co^{2+} are shown in the inset to Fig. 8E. The EC_{50} for Co^{2+} of D1049N and E1062Q were 72.4 μM and 126 μM, respectively, which were similar to the aforementioned EC_{50} for Co^{2+} of WT TRPM4 (57.5 μM, Table 1).

In all the constructs, 1 mM Co^{2+} was high enough to reach maximum decrease in the EC_{50} for Ca^{2+} (Fig. 8E). Therefore, we evaluated the EC_{50} for Ca^{2+} of all the constructs in the presence of 1 mM Co^{2+}, which is deemed to reflect the affinity of the 1st binding site for Ca^{2+} in the situation that the 2nd binding site is filled with Co^{2+}. The Ca^{2+} dose-response curves of D1049 and E1062 mutants were shifted to the right in comparison with that of WT TRPM4 and the mutations of E1062 showed a more pronounced effect than those of D1049 (Fig. 8F). The values of normalized current amplitudes of the all mutants were significantly different from those of WT at 0.1, 0.3, and/or 1 mM Ca^{2+}.

As summarized in Table 1, the mutations of D1049 and E1062 increased the values of EC_{50} for Ca^{2+} in the presence of 1 mM Co^{2+} rather than the values of EC_{50} for Co^{2+} as compared with WT TRPM4. Assuming that the EC_{50} for Ca^{2+} in the presence of 1 mM Co^{2+} reflects the affinity of the 1st binding site and the EC_{50} for Co^{2+} reflects affinity of the 2nd binding site, mutations of D1049 and E1062 most likely mainly affected the 1st binding site and decreased its Ca^{2+} sensitivity.

Mutations of D1049 and E1062 reduce the Ca^{2+} sensitivity in the presence of PIP_2 but do not

affect the sensitivity to PIP_2

PIP_2 is a membrane phosphoinositide that strongly enhances TRPM4 activity by increasing the Ca^{2+} sensitivity and shifting its voltage dependence towards negative potentials (16,17). It is important to reveal whether D1049 and E1062 play a role in the activation of TRPM4 by Ca^{2+} under a more physiological condition, i.e. in the presence of PIP_2. A water-soluble form of PIP_2, diC8-PI(4,5)P_2 (30 μM, CellSignals, Columbus, OH), was applied to the cytosolic perfusate. In the presence of PIP_2, the currents of WT TRPM4 and also D1049N and E1062Q mutants were evoked by lower concentrations of Ca^{2+} compared with the desensitized currents in the absence of PIP_2 (Fig.9A and compare with Fig. 5B). The Ca^{2+} dose-response curves of WT TRPM4, D1049N, and E1062Q in the presence of PIP_2 show that mutations of D1049 and E1062 decrease Ca^{2+} sensitivity which is elevated by PIP_2 (Fig. 9B). The EC_{50} for Ca^{2+} in the presence of PIP_2 are summarized in Table 1.

To exclude the possibility that the rightward shifts of Ca^{2+} dose-response curves of D1049N and E1062Q mutants compared with WT TRPM4 were due to reduction of sensitivities for PIP_2, the affinities for PIP_2 of the constructs were evaluated. Typical time-courses of the currents of WT TRPM4, D1049N, and E1062Q in the presence of several concentrations of PIP_2 are shown in Fig. 9C. The Ca^{2+} concentrations in perfusate were 0.1 mM, 0.3 mM, or 1 mM for WT TRPM4, D1049N, or E1062Q, respectively. They were close to the EC_{50} for Ca^{2+} of each construct in the presence of 30 μM PIP_2. The currents of all the constructs at +100 mV and also −100 mV were increased by PIP_2 (Fig. 9C). The dose-response curves for the effect of PIP_2 of WT TRPM4, D1049N, and E1062Q were similar (Fig. 9D). In particular, EC_{50} for PIP_2 of WT TRPM4, D1049N, and E1062Q were almost the same (Table 1).

These results suggest that D1049 and E1062 are necessary for the normal Ca^{2+} sensitivity maintained by binding with PIP_2 and moreover, PIP_2 probably increases the affinity for Ca^{2+} of the 1st binding site, which is related to D1049 and E1062 (Fig. 10). Negligible effects of the mutations on the sensitivity to PIP_2 indicate that the structure of PIP_2 binding site in the cytosolic C-terminal tail of TRPM4 (17) was not disturbed by the mutations.

DISCUSSION

The present study provides several new insights into the regulation of TRPM4 activity by intracellular Ca^{2+} as summarized in Fig. 10. First, there are at least two functionally different divalent cation binding sites in TRPM4 and/or associated proteins. One is the comparatively Ca^{2+}-specific binding site and the other is the binding site for Co^{2+}, Mn^{2+}, and Ni^{2+}. A binding of Ca^{2+} to the former (1st binding site) is required for the opening of TRPM4 channel. A binding of a divalent cation to the latter (2nd binding site) increases the Ca^{2+} sensitivity of the 1st binding site and make the channel less voltage-dependent as in the effect of PIP_2. The relief of inactivation at hyperpolarized membrane potentials has a great

influence on the channel activity at physiological membrane potentials. Next, the mutations of D1049 and E1062 decreased their Ca^{2+} sensitivity mainly by decreasing the Ca^{2+} sensitivity of the 1st binding site, and they had little effect on the affinities of the 2nd binding site and the PIP_2 binding site. Additionally, the modulations of voltage dependence by Co^2 and PIP_2 must have not been affected by the mutations because the inward currents of the mutants were increased by them as in WT TRPM4. Finally, the binding of Ca^{2+} to the 1st binding site (or at least a binding site other than the 2nd binding site) probably also makes the channel less voltage-dependent because the modulation of voltage dependence by high concentrations of Ca^{2+} was lost by the D1049N, D1049A, or E1062Q mutations, which had little effect on the modulation of voltage dependence through the 2nd binding site.

The reason why we conclude the mutations of E1062 and D1049 affected primarily the 1st binding site (comparatively Ca^{2+}-specific binding site) rather than the 2nd binding site (binding site for Co^{2+}) is because the mutations of these amino acid residues increased the EC_{50} for Ca^{2+} in the presence of Co^{2+} rather than the EC_{50} for Co^{2+}. For example, the D1049N mutant showed about 4 times larger EC_{50} for Ca^{2+} in the presence of 1 mM Co^{2+} than WT (shown in Fig. 8F and Table 1) but hardly affected the EC_{50} for Co^{2+} (WT: D1049N = 1: 1.3) (shown in Fig. 8E and Table 1). The former, EC_{50} for Ca^{2+} in the presence of 1 mM Co^{2+}, can be presumed to reflect the Ca^{2+} affinity of the 1st binding site for the following reason. One mM Co^{2+} is high enough to reduce EC_{50} for Ca^{2+} maximally, as shown in Fig. 8E, indicating that the effect of the binding of Co^{2+} to the 2nd binding site was saturated. Thus, the increases in the currents by Ca^{2+} in the presence of 1 mM Co^{2+} were supposed to be due to the Ca^{2+} binding to the 1st binding site. The latter, EC_{50} for Co^{2+}, which was calculated from the effect of the decreases in EC_{50} for Ca^{2+} caused by Co^{2+} shown in Fig. 8E, can be supposed to reflect the affinity for Co^{2+} of the 2nd binding site because the Co^{2+} affinity of the 1st binding site is inferred to be negligible.

Manganese and cobalt are essential mineral micronutrients for humans (37, 38). An important question is whether these divalent cations can regulate TRPM4 channel activity under physiological conditions. It was reported that the intracellular free Mn^{2+} concentration in ovine brain tissue was below 0.5 μM (39). We were unable to find literature in which an absolute intracellular free Co^{2+} concentration was measured under normal conditions. However, the serum concentration of cobalt in humans has been reported to be 1.8 nM, which is below that of manganese (7.3 nM) (40). Therefore, the intracellular concentration of free Co^{2+} may be similar to that of free Mn^{2+} or less. In the present study, more than 10 μM of Co^{2+} (Fig. 8E) or Mn^{2+} (data not shown) were necessary for the occurrences of their effects on TRPM4, which were over their inferred physiological intracellular concentrations. Additionally, because the effects of Co^{2+} and Mn^{2+} were reversible (e.g. Fig. 1A),

Co^{2+} and Mn^{2+} probably do not constitutively bind to TRPM4. Thus, although the increase of inward currents at negative potentials, which is elicited by binding of Co^{2+} or Mn^{2+} to the 2nd binding site, is advantageous for the control of physiological membrane potentials by TRPM4, there is no data clearly indicating that Co^{2+} and Mn^{2+} regulate TRPM4 activity under physiological conditions thus far.

The sensitivity to Mn^{2+} of TRPM4 might be important for the toxicity mechanisms of manganese. Excessive exposure or intake of manganese may lead to a condition known as manganism, which is caused by the preferential accumulation of manganese in brain areas rich in dopaminergic neurons (37). As manganese poisoning progresses, catecholamine levels decrease, most likely due to the loss of nigrostriatal dopaminergic neurons, and consequently, parkinsonian-like symptoms ensue (37). On the other hand, the pathological activation of TRPM4 in neurons has shown to mediate axonal and neuronal degeneration (13). Therefore, the contribution of TRPM4 activation by Mn^{2+} to the pathogenesis of manganism needs to be addressed.

If the 2nd binding site plays a physiological role in the regulation of TRPM4 activity, it should have affinity for Ca^{2+}. Although, as discussed above, the effect of high concentrations of Ca^{2+} on the voltage dependence is probably not due to the Ca^{2+} binding to the 2nd binding site, the following results might suggest that Ca^{2+} binds to the 2nd binding site and regulates the affinity of the 1st binding site. The differences in EC_{50} for Ca^{2+} between WT TRPM4 and the mutants of D1049 and E1062 in the absence of Co^{2+} and PIP_2 (shown in Fig. 5C and Table 1) were smaller than those in the presence of Co^{2+} or PIP_2 (shown in Fig. 8F and 9B and Table 1). If Ca^{2+} can bind to the 2nd binding site, the small differences in EC_{50} for Ca^{2+} between WT and the mutants in the absence of Co^{2+} and PIP_2 might be explained as follows. The Ca^{2+} affinity of the 1st binding site in the absence of Co^{2+} and PIP_2 might be near to (or perhaps in the case of the mutants of E1062, lower than) that of the 2nd binding site because the Ca^{2+} affinity of the 1st binding site is not increased by Co^{2+} nor PIP_2. Thus, the EC_{50} for Ca^{2+} in the absence of Co^{2+} and PIP_2 might be a result of the binding of Ca^{2+} to both binding sites and be more influenced by the Ca^{2+} affinity of the 2nd binding site than in the presence of Co^{2+} or PIP_2. The Ca^{2+} affinity of the 2nd binding site is less affected by the mutations than the 1st one. Therefore, the differences in EC_{50} for Ca^{2+} between WT TRPM4 and the mutants in the absence of Co^{2+} and PIP_2 were smaller than in the presence. Additionally, the Hill coefficient calculated from a fit of the Ca^{2+} dose-response curve for WT TRPM4 currents at +100 mV in the absence of Co^{2+} was 2.99 and that in the presence of 1 mM Co^{2+} was 1.45 (Table 1). This decrease of the Hill coefficient supports the idea that Ca^{2+} binds to more sites in the absence of Co^{2+} than its presence. However, even if Ca^{2+} can bind to the 2nd binding site at millimolar concentrations, it is unlikely that Ca^{2+} affects the TRPM4 function through the binding

to the 2nd binding site at physiological concentrations.

Our results do not deny the involvement of calmodulin in the regulation of TRPM4. The 2nd binding site might be calmodulin because Mn^{2+} has been shown to bind to and activate calmodulin (41-44). However, there are conflicting data. Co^{2+} and Ni^{2+} had the effects similar to Mn^{2+} on TRPM4 currents in the present study, but Co^{2+} and Ni^{2+} have been reported to have little or no effect on calmodulin (42,43). That implies the effects of the divalent cations on TRPM4 cannot be explained only by calmodulin. Furthermore, we cannot completely exclude the possibility that the single amino acid mutations near and in the TRP domain prevent the binding of calmodulin, the binding sites of which have been suggested to be located in the C-terminal region following the TRP domain (14). However, it should be noted that the mutations of D1049 and E1062 did not interfere with the binding of PIP_2. The PIP_2 binding site of TRPM4 has been shown to be located among the calmodulin binding sites in the C-terminal tail ((17), Fig. 5A). If the structure of the calmodulin binding sites were disturbed by the mutations, it is highly likely that the sensitivity for PIP_2 was likewise affected by the mutations.

Intriguingly, Mn^{2+}, Co^{2+}, and Ni^{2+}, the ionic radii of which are similar to each other and smaller than that of Ca^{2+} (Mn^{2+}: 0.80 Å, Co^{2+}: 0.74 Å, Ni^{2+}: 0.72 Å, and Ca^{2+}: 0.99 Å (20)), have been shown to be able to increase the apparent affinity of the BK channel for Ca^{2+} through binding to the E399-related low-affinity binding site (21,28). The mechanisms of how Mn^{2+}, Co^{2+}, and Ni^{2+} allosterically affect the affinity of the Ca^{2+} binding site in TRPM4 might be similar to those in the BK channel. Additionally, Mn^{2+}, Co^{2+}, and Ni^{2+} are the best activators of calcineurin, a serine/threonine protein phosphatase (45,46). Although calcineurin is also a calmodulin binding protein, Mn^{2+}, Co^{2+}, and Ni^{2+} were more potent activators of calcineurin than Ca^{2+} in the absence of calmodulin (47) through their binding to the divalent cation binding site in calcineurin (46). It would be interesting to examine whether calcineurin regulates TRPM4 or not. Moreover, information regarding the structures of divalent cation binding sites of the BK channel and calcineurin might be useful in searching for the binding site for Mn^{2+}, Co^{2+}, and Ni^{2+} in TPRM4.

D1049 and E1062, which are required for the normal Ca^{2+} sensitivity of TRPM4, are conserved in TRPM5, TRPM2, and TRPM8. TRPM5 is also a Ca^{2+}-sensitive channel and has been reported to be independent of calmodulin (15). Involvements of the comparable aspartate and glutamate of TRPM5 in its activation by Ca^{2+} should be addressed. TRPM2 is activated in a synergistic fashion by intracellular ADP-ribose and Ca^{2+} (48). It has been reported that the mutation of the calmodulin-binding domain, located in the N-terminal of TRPM2, made the channel nonfunctional (49). However, intriguingly, it has been also suggested that the Ca^{2+} binding sites of TRPM2 were located in intracellular deep crevices near the pore entrance (50). It is noteworthy that the TRP domain in TPRM2 is just

beneath the 6th transmembrane pore forming domain. TRPM8 has been reported to be desensitized in a Ca^{2+}-dependent manner (51). Although the desensitization by Ca^{2+} is considered to be due to the Ca^{2+}-mediated activation of PLC and subsequent PIP_2 hydrolysis near TRPM8 (51), the direct effects of Ca^{2+} through the comparable aspartate and glutamate of TRPM8 might be partially involved in the desensitization.

Our study demonstrated that the TRP domain of TRPM4 plays a pivotal role in determining Ca^{2+} sensitivity, which is a novel function of the TRP domain. As another example of functions of TRP domain in TRPM channels, it has been reported that the TRP domains of TRPM5 and TRPM8 channels are involved in the interaction with PIP_2 (19), which increases Ca^{2+} sensitivity of TRPM4 (16,17). However, the TRP box and TRP domain of TRPM4 were shown not to be the main determinants of PIP_2 action (17). Our data also consistently indicate that the mutation of D1049 and E1062 did not affect the sensitivity to PIP_2. Thus, the TRP domain of TRPM4 determines its Ca^{2+} sensitivity not by the modulating PIP_2 binding.

The simplest scenario how the mutations of D1049 and E1062 of TRPM4 reduced the Ca^{2+} sensitivity is that these two negative residues participate in the formation of a Ca^{2+} binding site. In this case, the contribution of D1049 to the formation of the 1st binding site may be smaller than that of E1062 because the effect on EC_{50} for Ca^{2+} of the mutation of D1049 was weaker than that of E1062. A second scenario is that the mutations disrupt the structure of a Ca^{2+} binding site, which is located elsewhere. At present, there is no conclusive data showing which scenario is the case. Clarification of the crystal structure of TRPM4 will help to understand the structure-function relationship. A third scenario is that the Ca^{2+} binding site is located in a different region and the mutations of D1049 and E1062 affected the allosteric mechanism that couples the signals of the Ca^{2+} binding with the channel opening. There are examples of such allosteric functions of the TRP domain. Amino acids I696 and W697 in the TRP box of TRPV1 are critical for the efficient coupling of stimulus sensing and gate opening (52). The TRP domain of TRPM8 was also indicated to be involved in translating the initial ligand-binding event to the allosteric conformational changes that open the channel independently from the effect of PIP_2 (53). However, in the present study, the EC_{50} for Ca^{2+} were increased by the D1049 or E1062 mutations of TRPM4. Therefore, it is more conceivable that the initial Ca^{2+}-binding event is inhibited by the mutations of D1049 or E1062 rather than the allosteric mechanisms in the case of TRPM4. Lastly, the mutations of D1049 and E1062 might have changed the amount of plasma membrane surface expression of the channels because the maximal current amplitudes of the mutants except E1062A, which were evoked by Ca^{2+} alone, were smaller than that of WT (Table 2). The maximal current amplitudes may reflect the expression level of the channel protein on the patch membrane although we cannot rule out the

possibility that the maximal current amplitudes are determined not only by the surface expression level but also by other unknown mechanisms. However, we measured the maximum reaction and analyzed the EC_{50} for divalent cations. Even if the maximal current amplitudes are changed according to the different surface expression levels of the channel proteins, the EC_{50} for divalent cations will not be affected. Thus, the change in surface expression level of the channel proteins does not affect our conclusion that the mutations of D1049 or E1062 reduce the Ca^{2+} sensitivity of TRPM4. Additionally, as shown in Table 2, the maximal current amplitudes of WT and mutants are not correlated to the Ca^{2+} sensitivities when E1062Q and E1062A are compared. Moreover, although the maximal current amplitudes of D1049N and E1062Q in the presence of PIP_2 were not significantly different from that of WT, the EC_{50} for Ca^{2+} of the mutants in the presence of PIP_2 were obviously larger than that of WT (Fig. 9B). Therefore, it is very unlikely that the surface expression level is the main determinant of the sensitivities to Ca^{2+}.

The mutations of D1049 and E1062 of TRPM4 also affected the voltage dependence. The voltage-independent conductance fraction and the currents amplitudes at −100 mV of WT TRPM4 were increased by the applications of Ca^{2+}, Co^{2+}, Mn^{2+}, Ni^{2+}, or PIP_2, which suggests that the inactivation of the currents at negative potentials was relieved by them. Though contrarily it has been reported that Ca^{2+} did not change the voltage dependence of TRPM4 (1,54), the Ca^{2+} concentrations at which the voltage dependence was affected in the present study (over 1 mM) were higher than those used in the articles (1,54). In contrast with WT TRPM4, the voltage-independent conductance fractions of D1049N, D1049A, and E1062Q mutants were not increased by Ca^{2+}. These results suggest not only that the voltage-sensing machinery can be regulated by Ca^{2+} but also that the mutations except E1062A disrupt the coupling between the signal of Ca^{2+} binding and the voltage-sensing machinery. It should be noted that the effects on the voltage dependence of Co^{2+} and PIP_2 were not eliminated by the any mutations of D1049 or E1062. These results indicate that the mutants do not lose the capability to regulate the voltage-sensing machinery. Furthermore, the WT-like behavior of E1062A mutant suggests that the expression level on the plasma membrane of the channels might account for the different responses of the voltage dependence by Ca^{2+}. As summarized in Table 2, the maximal current amplitudes of the mutants, which were evoked by Ca^{2+} alone, were significantly smaller than WT, except for E1062A. The surface expression level of E1062A, which may be the nearest to that of WT among the mutants, might cause the WT-like behavior of E1062A regarding the modification of voltage dependence by Ca^{2+}.

Finally, the time course of decrease in the current amplitudes after the first exposure to the calcium solution appears to vary between experiments even for the WT channel. Currently, we cannot clearly indicate the reason of the

variations. However, we assume that the variations were probably due to the variations in the initial ratio of the number of expressed channel proteins to the concentration of PIP_2 in a patch membrane. The concentrations of PIP_2 are probably similar among patch membranes. Thus, when the number of channel proteins is small and the ratio is low, the initial currents are large in comparison with the desensitized currents because the large percentage of channel proteins was initially potentiated by PIP_2. The loss of PIP_2 affected many channels so that the time course of the desensitization was sharp. When the number of channel proteins is large and the ratio is high, the opposite happens. Additionally, in some patch recordings, the currents increased slowly after patch excision (e.g. D1049N in Fig. 5B, WT in Fig. 9A). That's perhaps because the inside of the patch membrane was gradually opened after the vesicle formed. In those cases, the initial peak currents were not measured properly and thus the decrease in the current amplitudes appeared to be slow. On the other hand, the differences in the time course of the decrease in the current amplitudes between WT and mutants are probably mainly due to the difference in the Ca^{2+}-sensitivity among them.

In conclusion, the present study provides new insights to better understand the mechanisms underlying the activation of TRPM4. In particular, it demonstrated that the acidic amino acids near and in the TRP domain of TRPM4 play a pivotal role in the determination of Ca^{2+} sensitivity. If the crystal structure of the C-terminal tail of TRPM4 is revealed, it will be clarified whether the TRP domain of TRPM4 is a direct binding site for Ca^{2+} or not. At least, the functional observations by the present study will help to understand the correlation between the structure and function of TRPM4.

REFERENCES

1. Launay, P., Fleig, A., Perraud, A. L., Scharenberg, A. M., Penner, R., and Kinet, J. P. (2002) TRPM4 is a Ca^{2+}-activated nonselective cation channel mediating cell membrane depolarization. *Cell* **109**, 397-407
2. Zheng, J. (2013) Molecular mechanism of TRP channels. *Compr Physiol* **3**, 221-242
3. Guinamard, R., Salle, L., and Simard, C. (2011) The non-selective monovalent cationic channels TRPM4 and TRPM5. *Adv Exp Med Biol* **704**, 147-171
4. Mathar, I., Jacobs, G., Kecskes, M., Menigoz, A., Philippaert, K., and Vennekens, R. (2014) TRPM4. *Handb Exp Pharmacol* **222**, 461-487
5. Barbet, G., Demion, M., Moura, I. C., Serafini, N., Leger, T., Vrtovsnik, F., Monteiro, R. C., Guinamard, R., Kinet, J. P., and Launay, P. (2008) The calcium-activated nonselective cation channel TRPM4 is essential for the migration but not the maturation of dendritic cells. *Nat*

Immunol **9**, 1148-1156

6. Vennekens, R., Olausson, J., Meissner, M., Bloch, W., Mathar, I., Philipp, S. E., Schmitz, F., Weissgerber, P., Nilius, B., Flockerzi, V., and Freichel, M. (2007) Increased IgE-dependent mast cell activation and anaphylactic responses in mice lacking the calcium-activated nonselective cation channel TRPM4. *Nat Immunol* **8**, 312-320
7. Shimizu, T., Owsianik, G., Freichel, M., Flockerzi, V., Nilius, B., and Vennekens, R. (2009) TRPM4 regulates migration of mast cells in mice. *Cell Calcium* **45**, 226-232
8. Earley, S., Waldron, B. J., and Brayden, J. E. (2004) Critical role for transient receptor potential channel TRPM4 in myogenic constriction of cerebral arteries. *Circ Res* **95**, 922-929
9. Earley, S., Straub, S. V., and Brayden, J. E. (2007) Protein kinase C regulates vascular myogenic tone through activation of TRPM4. *Am J Physiol Heart Circ Physiol* **292**, H2613-2622
10. Kruse, M., Schulze-Bahr, E., Corfield, V., Beckmann, A., Stallmeyer, B., Kurtbay, G., Ohmert, I., Brink, P., and Pongs, O. (2009) Impaired endocytosis of the ion channel TRPM4 is associated with human progressive familial heart block type I. *J Clin Invest* **119**, 2737-2744
11. Liu, H., El Zein, L., Kruse, M., Guinamard, R., Beckmann, A., Bozio, A., Kurtbay, G., Megarbane, A., Ohmert, I., Blaysat, G., Villain, E., Pongs, O., and Bouvagnet, P. (2010) Gain-of-function mutations in TRPM4 cause autosomal dominant isolated cardiac conduction disease. *Circ Cardiovasc Genet* **3**, 374-385
12. Stallmeyer, B., Zumhagen, S., Denjoy, I., Duthoit, G., Hebert, J. L., Ferrer, X., Maugenre, S., Schmitz, W., Kirchhefer, U., Schulze-Bahr, E., and Guicheney, P. (2012) Mutational spectrum in the Ca^{2+}-activated cation channel gene TRPM4 in patients with cardiac conductance disturbances. *Hum Mutat* **33**, 109-117
13. Schattling, B., Steinbach, K., Thies, E., Kruse, M., Menigoz, A., Ufer, F., Flockerzi, V., Bruck, W., Pongs, O., Vennekens, R., Kneussel, M., Freichel, M., Merkler, D., and Friese, M. A. (2012) TRPM4 cation channel mediates axonal and neuronal degeneration in experimental autoimmune encephalomyelitis and multiple sclerosis. *Nature Medicine* **18**, 1805-1811
14. Nilius, B., Prenen, J., Tang, J., Wang, C., Owsianik, G., Janssens, A., Voets, T., and Zhu, M. X. (2005) Regulation of the Ca^{2+} sensitivity of the nonselective cation channel TRPM4. *J Biol Chem* **280**, 6423-6433
15. Hofmann, T., Chubanov, V., Gudermann, T., and Montell, C. (2003) TRPM5 is a voltage-modulated and Ca^{2+}-activated monovalent selective cation channel. *Curr Biol* **13**, 1153-1158
16. Zhang, Z., Okawa, H., Wang, Y., and Liman, E. R. (2005) Phosphatidylinositol 4,5-bisphosphate rescues TRPM4 channels from desensitization. *J Biol Chem* **280**, 39185-39192

17. Nilius, B., Mahieu, F., Prenen, J., Janssens, A., Owsianik, G., Vennekens, R., and Voets, T. (2006) The Ca^{2+}-activated cation channel TRPM4 is regulated by phosphatidylinositol 4,5-biphosphate. *EMBO J* **25**, 467-478
18. Ramsey, I. S., Delling, M., and Clapham, D. E. (2006) An introduction to TRP channels. *Annu Rev Physiol* **68**, 619-647
19. Rohacs, T., Lopes, C. M., Michailidis, I., and Logothetis, D. E. (2005) $PI(4,5)P_2$ regulates the activation and desensitization of TRPM8 channels through the TRP domain. *Nat Neurosci* **8**, 626-634
20. Zhou, Y., Zeng, X. H., and Lingle, C. J. (2012) Barium ions selectively activate BK channels via the Ca^{2+}-bowl site. *Proc Natl Acad Sci U S A* **109**, 11413-11418
21. Zeng, X. H., Xia, X. M., and Lingle, C. J. (2005) Divalent cation sensitivity of BK channel activation supports the existence of three distinct binding sites. *J Gen Physiol* **125**, 273-286
22. Nilius, B., Prenen, J., Voets, T., and Droogmans, G. (2004) Intracellular nucleotides and polyamines inhibit the Ca^{2+}-activated cation channel TRPM4b. *Pflugers Arch* **448**, 70-75
23. Sunose, H., Ikeda, K., Saito, Y., Nishiyama, A., and Takasaka, T. (1993) Nonselective cation and Cl channels in luminal membrane of the marginal cell. *Am J Physiol* **265**, C72-78
24. Takeuchi, S., Marcus, D. C., and Wangemann, P. (1992) Ca^{2+}-activated nonselective cation, maxi K^+ and Cl^- channels in apical membrane of marginal cells of stria vascularis. *Hear Res* **61**, 86-96
25. Sakuraba, M., Murata, J., Teruyama, R., Kamiya, K., Yamaguchi, J., Okano, H., Uchiyama, Y., and Ikeda, K. (2014) Spatiotemporal expression of TRPM4 in the mouse cochlea. *J Neurosci Res* **92**, 1409-1418
26. Yoo, J. C., Yarishkin, O. V., Hwang, E. M., Kim, E., Kim, D. G., Park, N., Hong, S. G., and Park, J. Y. (2010) Cloning and characterization of rat transient receptor potential-melastatin 4 (TRPM4). *Biochem Biophys Res Commun* **391**, 806-811
27. Suzuki, K., Hattori, T., and Yamasaki, K. (1968) The stability constants of o-phenylenedioxydiacetic acid chelates of bivalent metals. *J. Inorg. Nucl. Chem.* **30**, 161-166
28. Oberhauser, A., Alvarez, O., and Latorre, R. (1988) Activation by divalent cations of a Ca^{2+}-activated K^+ channel from skeletal muscle membrane. *J Gen Physiol* **92**, 67-86
29. Simon, F., Leiva-Salcedo, E., Armisen, R., Riveros, A., Cerda, O., Varela, D., Eguiguren, A. L., Olivero, P., and Stutzin, A. (2010) Hydrogen peroxide removes TRPM4 current desensitization conferring increased vulnerability to necrotic cell death. *J Biol Chem* **285**, 37150-37158
30. Amarouch, M. Y., Syam, N., and Abriel, H. (2013) Biochemical, single-channel, whole-cell patch clamp, and pharmacological analyses of endogenous TRPM4 channels in HEK293 cells. *Neurosci Lett* **541**, 105-110

31. Nadler, M. J., Hermosura, M. C., Inabe, K., Perraud, A. L., Zhu, Q., Stokes, A. J., Kurosaki, T., Kinet, J. P., Penner, R., Scharenberg, A. M., and Fleig, A. (2001) LTRPC7 is a Mg.ATP-regulated divalent cation channel required for cell viability. *Nature* **411**, 590-595
32. Kozak, J. A., Matsushita, M., Nairn, A. C., and Cahalan, M. D. (2005) Charge screening by internal pH and polyvalent cations as a mechanism for activation, inhibition, and rundown of TRPM7/MIC channels. *J Gen Physiol* **126**, 499-514
33. Matsushita, M., Kozak, J. A., Shimizu, Y., McLachlin, D. T., Yamaguchi, H., Wei, F. Y., Tomizawa, K., Matsui, H., Chait, B. T., Cahalan, M. D., and Nairn, A. C. (2005) Channel function is dissociated from the intrinsic kinase activity and autophosphorylation of TRPM7/ChaK1. *J Biol Chem* **280**, 20793-20803
34. Ullrich, N. D., Voets, T., Prenen, J., Vennekens, R., Talavera, K., Droogmans, G., and Nilius, B. (2005) Comparison of functional properties of the Ca^{2+}-activated cation channels TRPM4 and TRPM5 from mice. *Cell Calcium* **37**, 267-278
35. Sumoza-Toledo, A., and Penner, R. (2011) TRPM2: a multifunctional ion channel for calcium signalling. *J Physiol* **589**, 1515-1525
36. Liu, Y., and Qin, N. (2011) TRPM8 in health and disease: cold sensing and beyond. *Adv Exp Med Biol* **704**, 185-208
37. Avila, D. S., Puntel, R. L., and Aschner, M. (2013) Manganese in health and disease. *Met Ions Life Sci* **13**, 199-227
38. Yamada, K. (2013) Cobalt: its role in health and disease. *Met Ions Life Sci* **13**, 295-320
39. Wedler, F. C., Denman, R. B., and Roby, W. G. (1982) Glutamine synthetase from ovine brain is a manganese(II) enzyme. *Biochemistry* **21**, 6389-6396
40. Forrer, R., Gautschi, K., and Lutz, H. (2001) Simultaneous measurement of the trace elements Al, As, B, Be, Cd, Co, Cu, Fe, Li, Mn, Mo, Ni, Rb, Se, Sr, and Zn in human serum and their reference ranges by ICP-MS. *Biol Trace Elem Res* **80**, 77-93
41. Wolff, D. J., Poirier, P. G., Brostrom, C. O., and Brostrom, M. A. (1977) Divalent cation binding properties of bovine brain Ca^{2+}-dependent regulator protein. *J Biol Chem* **252**, 4108-4117
42. Chao, S. H., Suzuki, Y., Zysk, J. R., and Cheung, W. Y. (1984) Activation of calmodulin by various metal cations as a function of ionic radius. *Mol Pharmacol* **26**, 75-82
43. Habermann, E., Crowell, K., and Janicki, P. (1983) Lead and other metals can substitute for Ca^{2+} in calmodulin. *Arch Toxicol* **54**, 61-70
44. Milos, M., Comte, M., Schaer, J. J., and Cox, J. A. (1989) Evidence for four capital and six auxiliary cation-binding sites on calmodulin: divalent cation interactions monitored by direct binding and microcalorimetry. *J Inorg Biochem* **36**, 11-25

45. Wolff, D. J., and Sved, D. W. (1985) The divalent cation dependence of bovine brain calmodulin-dependent phosphatase. *J Biol Chem* **260**, 4195-4202
46. Ping, L., Ke, Z., Benqiong, X., and Qun, W. (2004) Effect of metal ions on the activity of the catalytic domain of calcineurin. *Biometals* **17**, 157-165
47. Pallen, C. J., and Wang, J. H. (1984) Regulation of calcineurin by metal ions. Mechanism of activation by Ni^{2+} and an enhanced response to Ca^{2+}/calmodulin. *J Biol Chem* **259**, 6134-6141
48. Faouzi, M., and Penner, R. (2014) TRPM2. *Handb Exp Pharmacol* **222**, 403-426
49. Du, J., Xie, J., and Yue, L. (2009) Intracellular calcium activates TRPM2 and its alternative spliced isoforms. *Proc Natl Acad Sci U S A* **106**, 7239-7244
50. Csanady, L., and Torocsik, B. (2009) Four Ca^{2+} ions activate TRPM2 channels by binding in deep crevices near the pore but intracellularly of the gate. *J Gen Physiol* **133**, 189-203
51. Almaraz, L., Manenschijn, J. A., de la Pena, E., and Viana, F. (2014) TRPM8. *Handb Exp Pharmacol* **222**, 547-579
52. Gregorio-Teruel, L., Valente, P., Gonzalez-Ros, J. M., Fernandez-Ballester, G., and Ferrer-Montiel, A. (2014) Mutation of I696 and W697 in the TRP box of vanilloid receptor subtype I modulates allosteric channel activation. *J Gen Physiol* **143**, 361-375
53. Bandell, M., Dubin, A. E., Petrus, M. J., Orth, A., Mathur, J., Hwang, S. W., and Patapoutian, A. (2006) High-throughput random mutagenesis screen reveals TRPM8 residues specifically required for activation by menthol. *Nat Neurosci* **9**, 493-500
54. Nilius, B., Prenen, J., Droogmans, G., Voets, T., Vennekens, R., Freichel, M., Wissenbach, U., and Flockerzi, V. (2003) Voltage dependence of the Ca^{2+}-activated cation channel TRPM4. *J Biol Chem* **278**, 30813-30820

FOOTNOTES

The authors declare no conflict of interest. The work was supported by a grant from the Takeda Science Foundation (to S. Y.) and the Tsukada grant for Niigata University Medical Research (to S. Y.).

FIGURE LEGENDS

TABLE 1. EC_{50} and Hill coefficients for Ca^{2+}, Co^{2+}, and PIP_2 of wild-type TRPM4 and mutants (D1049A, D1049N, E1062A, and E1062Q). EC_{50} and Hill coefficients for Ca^{2+} were determined without additional conditions or also in the presence of 1 mM Co^{2+} or 30 μM diC8-PI(4,5)P_2 (PIP_2). EC_{50} and Hill coefficients for Co^{2+} were calculated from the decrease of EC_{50} for Ca^{2+} by the simultaneous

application of Co^{2+}, shown in Fig. 8E. The EC_{50} and Hill coefficients for PIP_2 were evaluated in the presence of Ca^{2+}, shown in Fig. 9D. The Ca^{2+} concentrations used for wild-type (WT) TRPM4, D1049N, and E1062Q were 100 μM, 300 μM, and 1 mM Ca^{2+}, respectively. The ratios of the EC_{50} of mutants to that of WT TRPM4 are shown in the parentheses. The current amplitudes at +100 mV were used for the calculation.

TABLE 2. Maximal current amplitudes of wild-type TRPM4 and mutants (D1049A, D1049N, E1062A, and E1062Q). The maximal current amplitudes at +100 mV in the presence of only Ca^{2+}, Ca^{2+} and 1 mM Co^{2+}, or Ca^{2+} and 30 μM PIP_2 are shown. The Ca^{2+} concentrations, at which the current amplitudes reached maximum, are listed next to the current amplitudes. Shown are the mean ±S.E. from 3-7 patch recordings. * $P < 0.05$, ** $P < 0.01$ vs. WT (Dunnett's test).

FIGURE 1. Intracellular Mn^{2+}, Co^{2+}, and Ni^{2+} potentiate TRPM4 channel activity. *A*, a representative time course of TRPM4 currents at +100 mV (filled circles) and −100 mV (open squares) in an inside-out patch using the voltage-ramp protocol. The arrow indicates the onset of inside-out mode. *B*, traces of inside-out currents evoked by ramp-pulse. The letters correspond to those described in A. (inset) *I-V* curves recorded from a mock transfected cell when the bath solutions were a Ca^{2+}-free solution (EGTA), a solution containing 1 mM Ca^{2+}, one containing 1 m Ca^{2+} and 1 mM Co^{2+}, or one containing 1 mM Ca^{2+} and 10 mM Mn^{2+}. *C*, averaged values of normalized current amplitudes showing the activation by the application of 1 mM divalent cations (Ca^{2+}, Ni^{2+}, Co^{2+}, and Mn^{2+}) in the presence of 1 mM Ca^{2+}. The current amplitudes at +100 mV (shaded bars) and −100 mV (unshaded bars) were normalized to the current amplitude recorded in the presence of 1 mM Ca^{2+} right before exposure to the other divalent cations.. Shown are mean ±S.E. **: $P < 0.01$ vs. currents evoked by 1 mM Ca^{2+}. n = 8-10. *D*, applications of 1 mM Ni^{2+}, Mn^{2+}, and Co^{2+} make TRPM4 voltage-independent. The horizontal axis is the membrane potential and the vertical axis is the chord conductance normalized to that at +100 mV. Shown are the mean ±S.E. from 8-10 patch recordings. The lines are fits to the Boltzmann equation.

FIGURE 2. TRPM4 currents potentiated by Co^{2+} are inhibited by a TRPM4 inhibitor, flufenamic acid. *A*, a typical time-course of TRPM4 channel currents at +100 mV (filled circles) and −100 mV (open squares) when 100 μM flufenamic acid (FA) was applied to the cytosolic side of TRPM4. FA was added to the perfusate which contained 1 mM Ca^{2+} with and without 1 mM Co^{2+}. *B*, averaged values of normalized current amplitudes at +100 mV (shaded bars) and −100 mV (unshaded bars). The currents were normalized to the current amplitude recorded in the presence of 1 mM Ca^{2+} right before exposure to the FA or 1 mM Co^{2+}. FA inhibited TRPM4 currents significantly regardless of whether TRPM4 currents

were potentiated by Co^{2+}. *: $P < 0.05$, **: $P < 0.01$. $n = 4$ or 6.

FIGURE 3. Effects of other divalent cation on TRPM4 activity. *A*, a typical time course of TRPM4 channel currents at +100 mV (filled circles) and −100 mV (open squares). One mM of Mg^{2+} (a), Ba^{2+}, Sr^{2+} (b), Cd^{2+}, or Zn^{2+} (c) was applied to the intracellular side of the patch membrane with 1 mM of Ca^{2+}. *B*, summary of the change in current amplitudes by the application of 1 mM divalent cations (Mg^{2+}, Ba^{2+}, Sr^{2+}, Cd^{2+}, or Zn^{2+}) in the presence of 1 mM Ca^{2+}. The current amplitudes at +100 mV (shaded bars) and −100 mV (unshaded bars) were normalized to the current amplitude recorded in the presence of 1 mM Ca^{2+} right before exposure to the other divalent cations. *: $P < 0.05$, **: $P < 0.01$ vs. currents evoked by 1 mM Ca^{2+}. $n = 4$-11.

FIGURE 4. Ca^{2+} dependence of the effects of Mn^{2+}, Co^{2+}, and Ni^{2+}. *A* (a), a representative time course of TRPM4 currents at +100 mV (filled circles) and −100 mV (open squares) showing that neither 1 mM Co^{2+}, Ni^{2+}, nor Mn^{2+} evoked any currents when the Ca^{2+} was chelated by 145 mM fluoride. (b), summary of the normalized currents at +100 mV (shaded bars) and −100 mV (unshaded bars). Shown are mean ±S.E. The normalized current amplitudes in the presence of Co^{2+}, Ni^{2+}, or Mn^{2+} were not significantly different from those under the Ca^{2+}-free condition using EGTA. $n = 3$ or 4. *B* (a), a typical time course of TRPM4 currents when the free Ca^{2+} and Co^{2+} concentrations were adjusted to 0 or 1 mM using a chelating agent, o-phenylenedioxydiacetic acid (o-PDDA, 6 mM). (b), summary of the normalized currents at +100 mV (shaded bars) and −100 mV (unshaded bars). Shown are mean ±S.E. The normalized current amplitudes in the presence of Co^{2+} (1 mM) were not significantly different from those under the Ca^{2+}-free condition using o-PDDA. Application of Co^{2+} (1 mM) in the presence of Ca^{2+} (1 mM) increased TRPM4 current amplitudes significantly. **: $P < 0.01$. $n = 5$. *C*, a diagram of two divalent cation binding sites of TRPM4 and their agonists. As the effects of Co^{2+}, Mn^{2+}, and Ni^{2+} are dependent on Ca^{2+}, it is suggested that there are at least two divalent cation binding sites in TRPM4. The 1st binding site is sensitive to Ca^{2+} but insensitive to Co^{2+}, Mn^{2+}, and Ni^{2+}. Accordingly, it is relatively Ca^{2+}-specific. The 2nd binding site is sensitive to Co^{2+}, Mn^{2+}, and Ni^{2+}.

FIGURE 5. Mutations of the acidic amino acids (D1049 and E1062) near and in the TRP domain reduce Ca^{2+} sensitivity. *A*, positions of the acidic amino acids which were mutated. (Upper) predicted membrane topology of TRPM4 and the binding sites for PIP_2 and calmodulin (CaM) in the C-terminal tail are illustrated. (Lower) an alignment of cDNA sequences around the TRP domain of rat TRPM channels is shown. The aspartate (D1049) and the glutamate (E1062) near and in the TRP domain of rat TRPM4 are conserved in rat TRPM5 (Genbank accession #NP_001178825.1), TRPM2 (#NP_001011559.1), and

TRPM8 (#NP_599198.2) but not in TRPM1 (#NP_001032823.1), TRPM3 (NP_001178491.1), TRPM6 (#XP_219747.6), nor TRPM7 (NP_446157.2). *B*, typical time courses of currents of WT TRPM4 and mutants (D1049N, D1049A, E1062Q, and E1062A). Intracellular Ca^{2+} concentration was increased from 0 to 30 mM. Arrows indicate the onset of inside-out mode. Application of 1 mM Co^{2+} potentiated all mutants. *C*, dose-response curves for the effect of intracellular Ca^{2+} on WT TRPM4 and mutants. Shown are the mean ±S.E. from 3-7 patch recordings. Current amplitudes are normalized to the maximum currents. The lines are fits to the Hill equation. *$P < 0.05$, ** $P < 0.01$ vs. WT (Dunnett's test).

FIGURE 6. Mn^{2+} and Ni^{2+} potentiate the currents of the mutants. Representative time courses of currents of D1049N (A), D1049A (B), E1062Q (C), and E1062A (D) at +100 mV (filled circles) and −100 mV (open squares). One mM of Mn^{2+}, Co^{2+}, Ni^{2+}, or Ca^{2+} was applied to the intracellular side of the patch membrane with 1 mM of Ca^{2+}.

FIGURE 7. Mutations of the acidic amino acids (D1049N, D1049A, and E1062Q) alter voltage dependence. *A*, typical *I-V* curves of Ca^{2+}-dependent currents recorded from the inside-out patch membrane expressing WT TRPM4 and mutants (D1049N, D1049A, E1062Q, and E1062A). The Ca^{2+}-dependent currents were obtained by subtracting the currents under the Ca^{2+}-free condition from the currents evoked by 3 mM Ca^{2+}. *B*, summary of the ratio of currents at −100 mV to those at +100 mV. The ratios of D1049N, D1049A, and E1062Q mutants were significantly different with that of WT TRPM4. Shown are the mean ±S.E. from 4-6 patch recordings. *: $P < 0.05$, **: $P < 0.01$ (Dunnett's test). *C*, changes of chord conductance of WT TRPM4 and mutants by intracellular Ca^{2+} concentrations. The values are normalized to the conductance at +100 mV. Shown are the mean ±S.E. from 3-6 patch recordings. The lines are fits to the Boltzmann equation.

FIGURE 8. Co^{2+} increases the Ca^{2+} sensitivity of the apparently Ca^{2+}-specific (1st) binding site and the mutations of D1049 and E1062 decrease the sensitivity to divalent cations of the 1st binding site rather than that of the Co^{2+} binding site. *A*, typical time courses of WT TRPM4 currents, showing that the Ca^{2+} sensitivity is increased by the simultaneous application of 1 mM Co^{2+} (a), Mn^{2+} (b), or Ni^{2+} (c). *B-D*, dose-response curves for the effect of intracellular Ca^{2+} on WT TRPM4 (B), D1049N (C), and E1062Q (D) mutants in the absence or presence of Co^{2+} (0.01 mM to 1 mM). Shown are the mean ±S.E. from 3-9 patch recordings. The lines are fits to the Hill equation. *E*, application of Co^{2+} reduces EC_{50} for the activation by Ca^{2+} of WT TRPM4 (black circles), D1049N (red triangles), and E1062Q (blue squares) mutants. The horizontal axis shows Co^{2+} concentration. The vertical axis shows the EC_{50} for Ca^{2+}. The lines are fit to the pseudo Hill equation. (inset) EC_{50} for Ca^{2+} are normalized to that in the absence of Co^{2+}

for the sake of comparison of EC_{50} for Co^{2+} between WT TRPM4 and the mutants. *F*, dose-response curves for the effect of intracellular Ca^{2+} on WT TRPM4 (black circles), D1049N (blue triangles), D1049A (red inverted triangles), E1062Q (green diamonds), and E1062A (pink squares) mutants in the presence of 1 mM Co^{2+}. Shown are the mean ±S.E. from 3-10 patch recordings. The lines are fits to the Hill equation. **P* < 0.05, ** *P* < 0.01 vs. WT (Dunnett's test).

FIGURE 9. D1049N and E1062Q mutants showed lower sensitivity to Ca^{2+} than WT TRPM4 in the presence of PIP_2. *A*, typical time courses of currents of WT TRPM4 and mutants (D1049N and E1062Q) in the presence of 30 μM diC8-PI(4,5)P_2 (PIP_2). Intracellular Ca^{2+} concentration was raised from 0 to 10 mM. *B*, dose-response curves for the effect of intracellular Ca^{2+} on TRPM4 and mutants (D1049N and E1062Q) in the presence of 30 μM diC8-PI(4,5)P_2. Current amplitudes are normalized to the maximum currents. Shown are the mean ±S.E. from 3-5 patch recordings. The lines are fits to the Hill equation. **P* < 0.05, ** *P* < 0.01 vs. WT (Dunnett's test). Data at 0.3 mM Ca^{2+} were not statistically analyzed because the value of WT at the concentration was not measured. *C*, typical time courses of currents of WT TRPM4 and mutants (D1049N and E1062Q) when the concentration of diC8-PI(4,5)P_2 was increased from 3 to 60 μM. Intracellular Ca^{2+} concentrations were 100 μM, 300 μM, and 1 mM for WT TRPM4, D1049N mutant, and E1062Q mutant, respectively. *D*, dose-response curves for the effect of intracellular diC8-PI(4,5)P_2 on WT TRPM4 and mutants (D1049N and E1062Q). Current amplitudes are normalized to the maximum currents. Shown are the mean ±S.E. from 3-6 patch recordings. The lines are fits to the Hill equation.

FIGURE 10. Suggested regulatory mechanisms of the TRPM4 activation. The bindings of divalent cation to the 2nd binding site and the binding of PIP_2 to its binding site have similar effects. They increase Ca^{2+} sensitivity of the 1st binding site and make TRPM4 less voltage-dependent. Hence, these sites function as regulatory sites. The binding of Ca^{2+} to the 1st binding site opens the channel and also affects voltage dependence. The mutations in D1049 and E1062 attenuate the Ca^{2+} sensitivity of the 1st binding site and inhibit the effects on the voltage dependence through the 1st Ca^{2+} binding site although the mutations hardly affect the function of the regulatory sites.

EC_{50} (mutants/WT), Hill coefficient

	Ca^{2+}	Ca^{2+} w/ Co^{2+}	Co^{2+}	Ca^{2+} w/ PIP_2	PIP_2
TRPM4 WT	0.96 mM (1.0), 2.99	107 μM (1.0), 1.45	57.5 μM (1.0), 1.04	42.2 μM (1.0), 1.26	9.96 μM (1.0), 2.82
D1049N	1.17 mM (1.2), 6.74	417 μM (3.9), 2.82	72.4 μM (1.3), 1.78	288 μM (6.8), 2.68	9.80 μM (1.0), 1.83
D1049A	1.21 mM (1.3), 3.62	304 μM (2.8), 1.41	-	-	-
E1062Q	3.65 mM (3.8), 4.24	1067 μM (10.0), 2.10	126 μM (2.2), 2.42	809 μM (19.0), 4.47	9.95 μM (1.0), 2.58
E1062A	2.78 mM (2.9), 3.23	856 μM (8.0), 1.18	-	-	-

Table 1, Yamaguchi, *et al.*

Maximal current amplitudes

	only Ca^{2+}		in the presence of Co^{2+}		in the presence of PIP_2	
	Currents (pA)	$[Ca^{2+}]_i$	Currents (pA)	$[Ca^{2+}]_i$	Currents (pA)	$[Ca^{2+}]_i$
TRPM4 WT	4134 ±818	3 mM	2870 ±544	3 mM	5420 ±636	1 mM
D1049N	** 617 ±416	3 mM	* 904 ±298	3 mM	4032 ±486	1 mM
D1049A	** 882 ±196	10 mM	* 1020 ±541	3 mM	-	-
E1062Q	** 113 ±17	10 mM	* 468 ±123	10 mM	3563 ±709	3 mM
E1062A	2471 ±1305	10 mM	3606 ±815	30 mM	-	-

Table 2, Yamaguchi, *et al.*

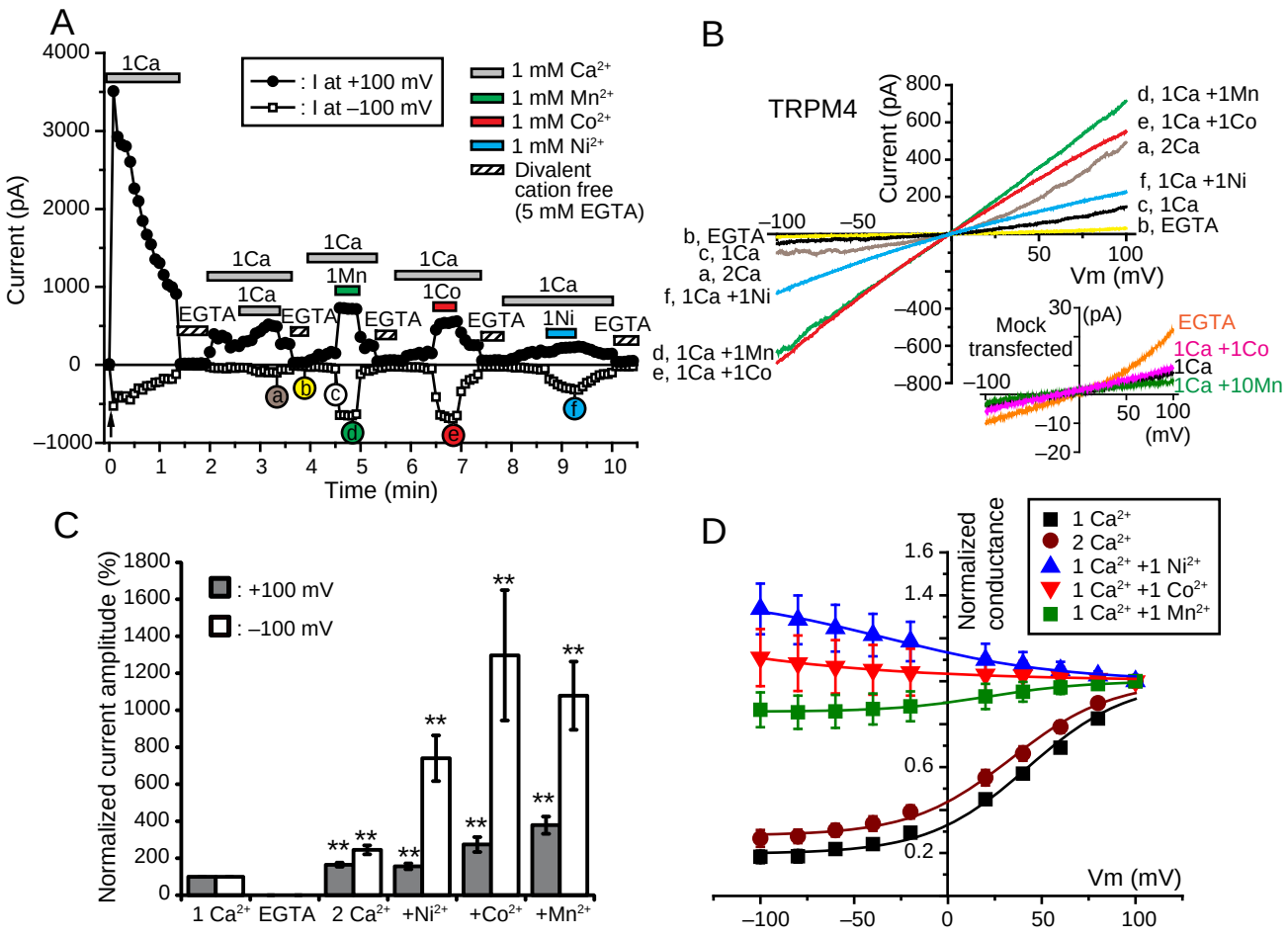

Figure 1, Yamaguchi, *et al.*

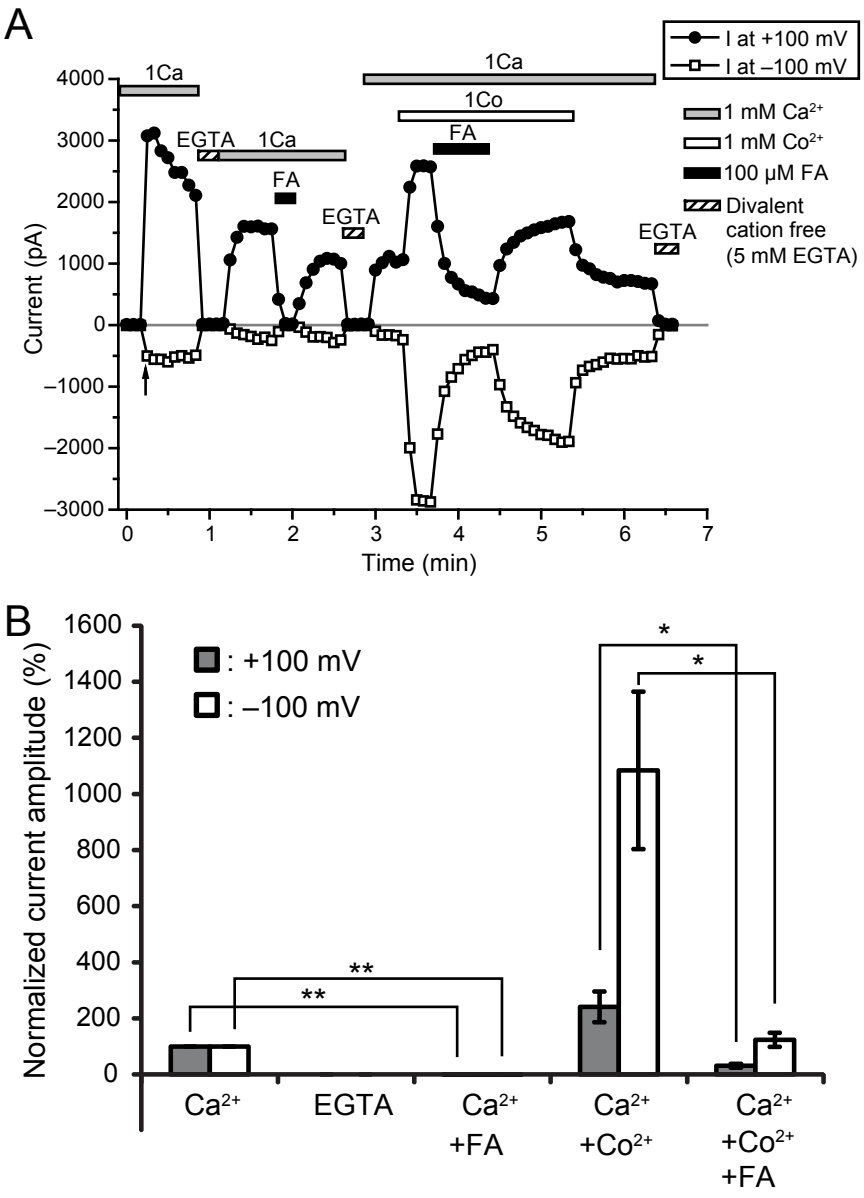

Figure 2, Yamaguchi, *et al.*

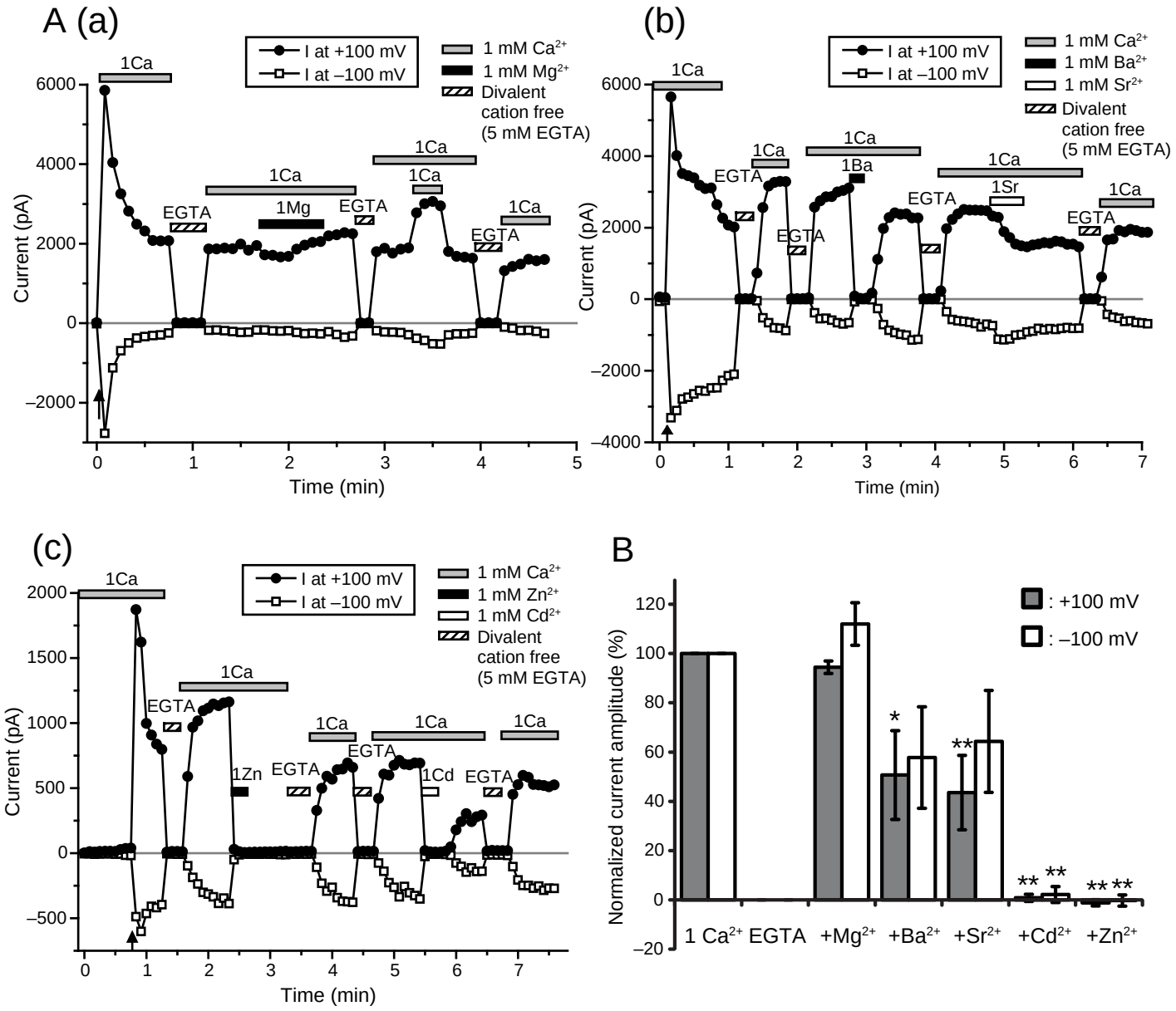

Figure 3, Yamaguchi, *et al.*

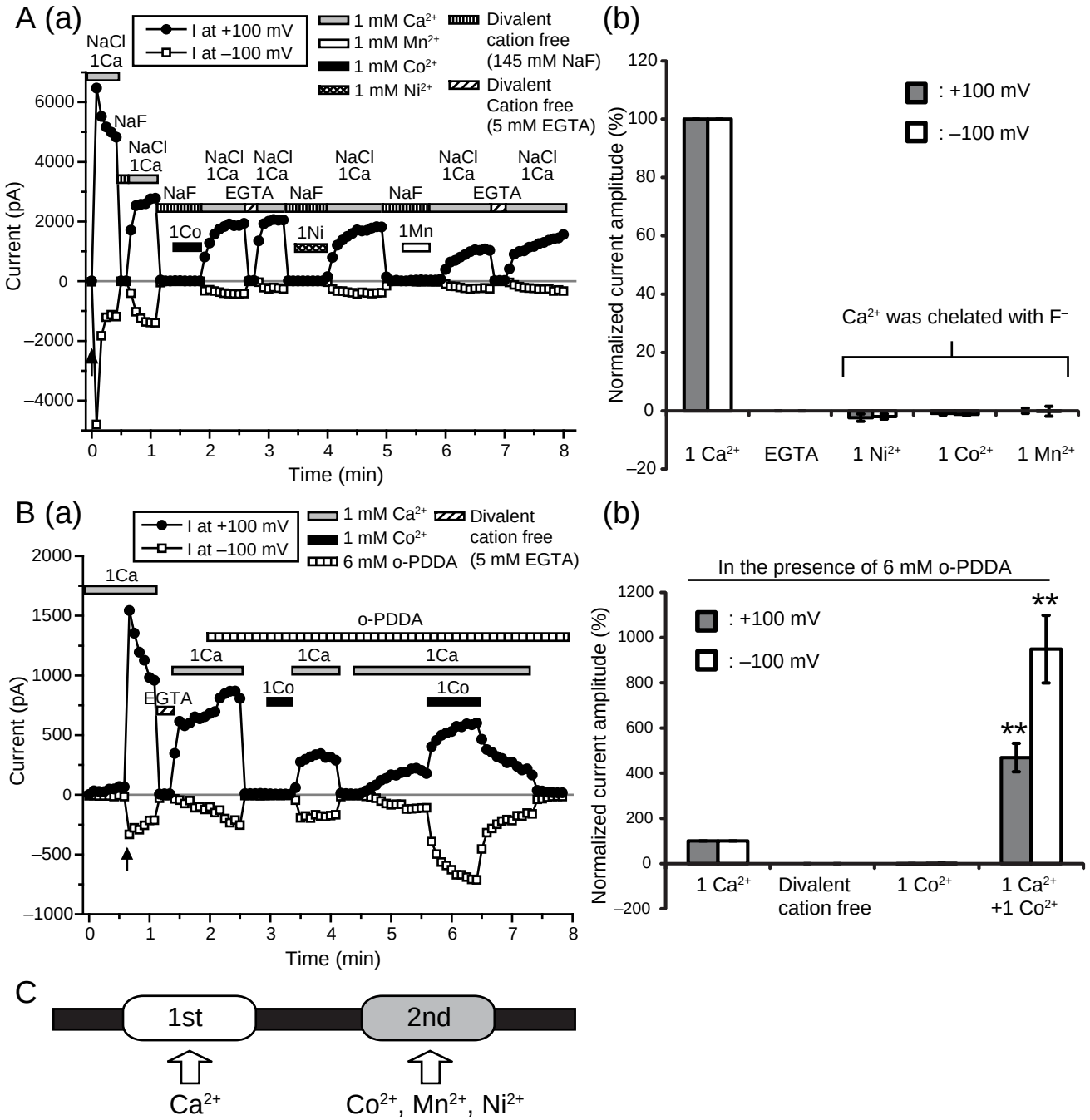

Figure 4, Yamaguchi, *et al.*

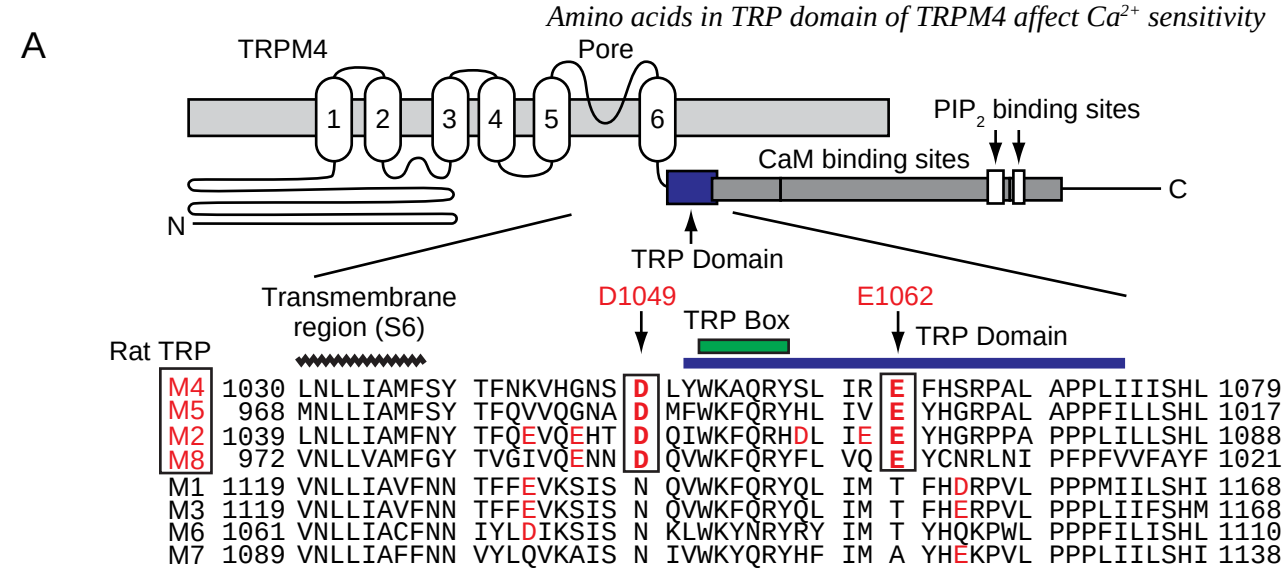

Figure 5, Yamaguchi, *et al.*

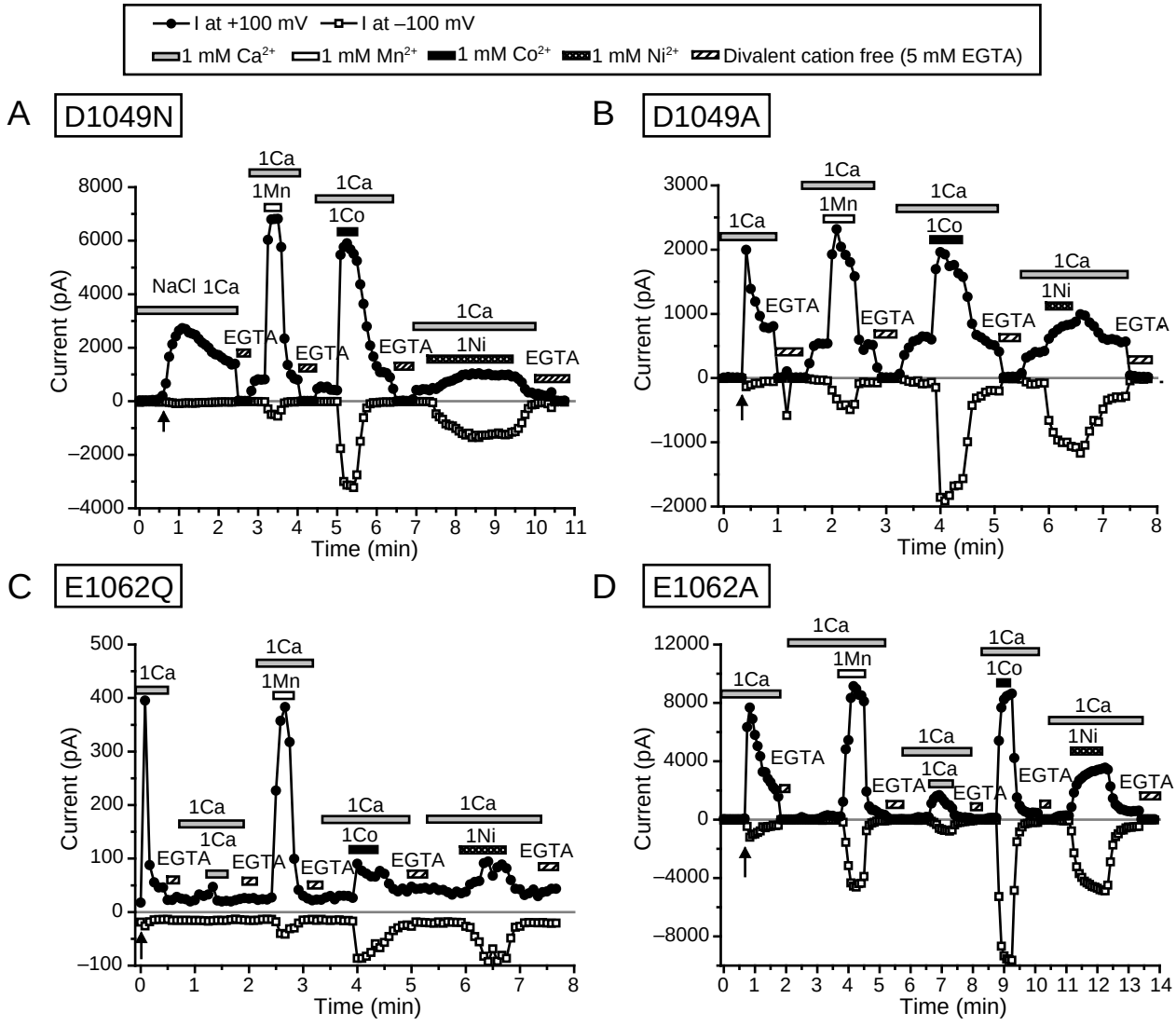

Figure 6, Yamaguchi, *et al.*

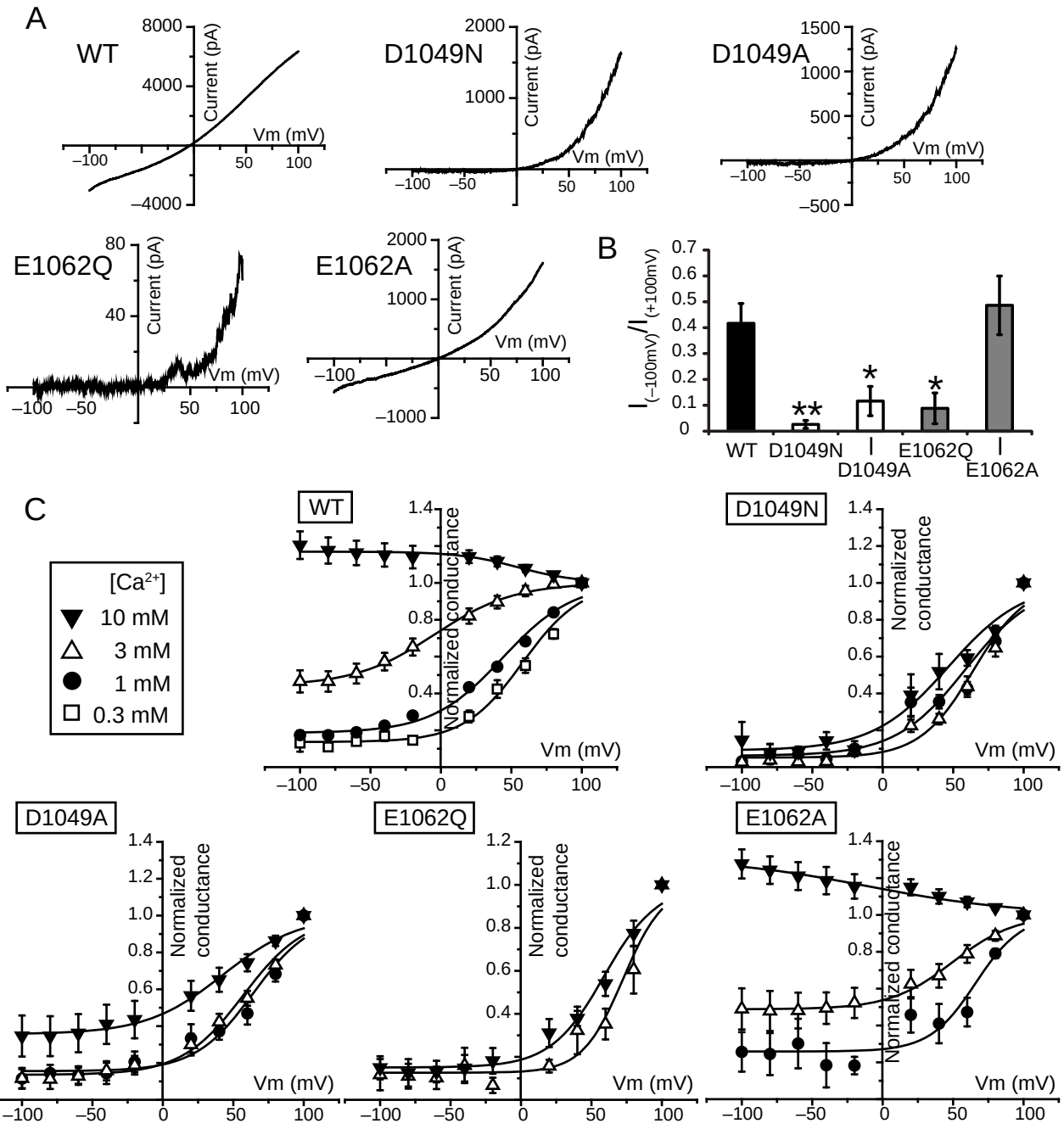

Figure 7, Yamaguchi, *et al.*

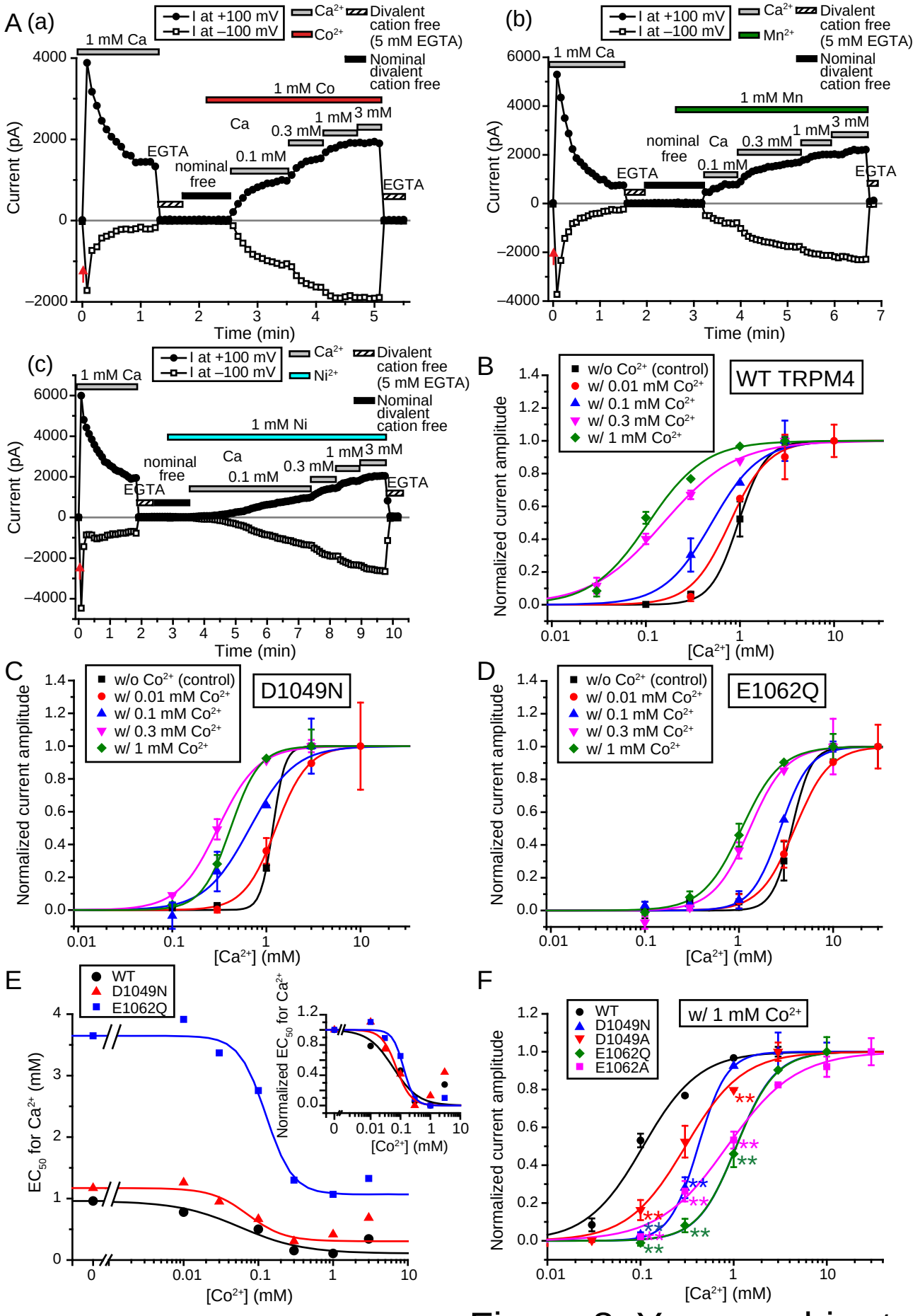

 Figure 8, Yamaguchi, *et al.*

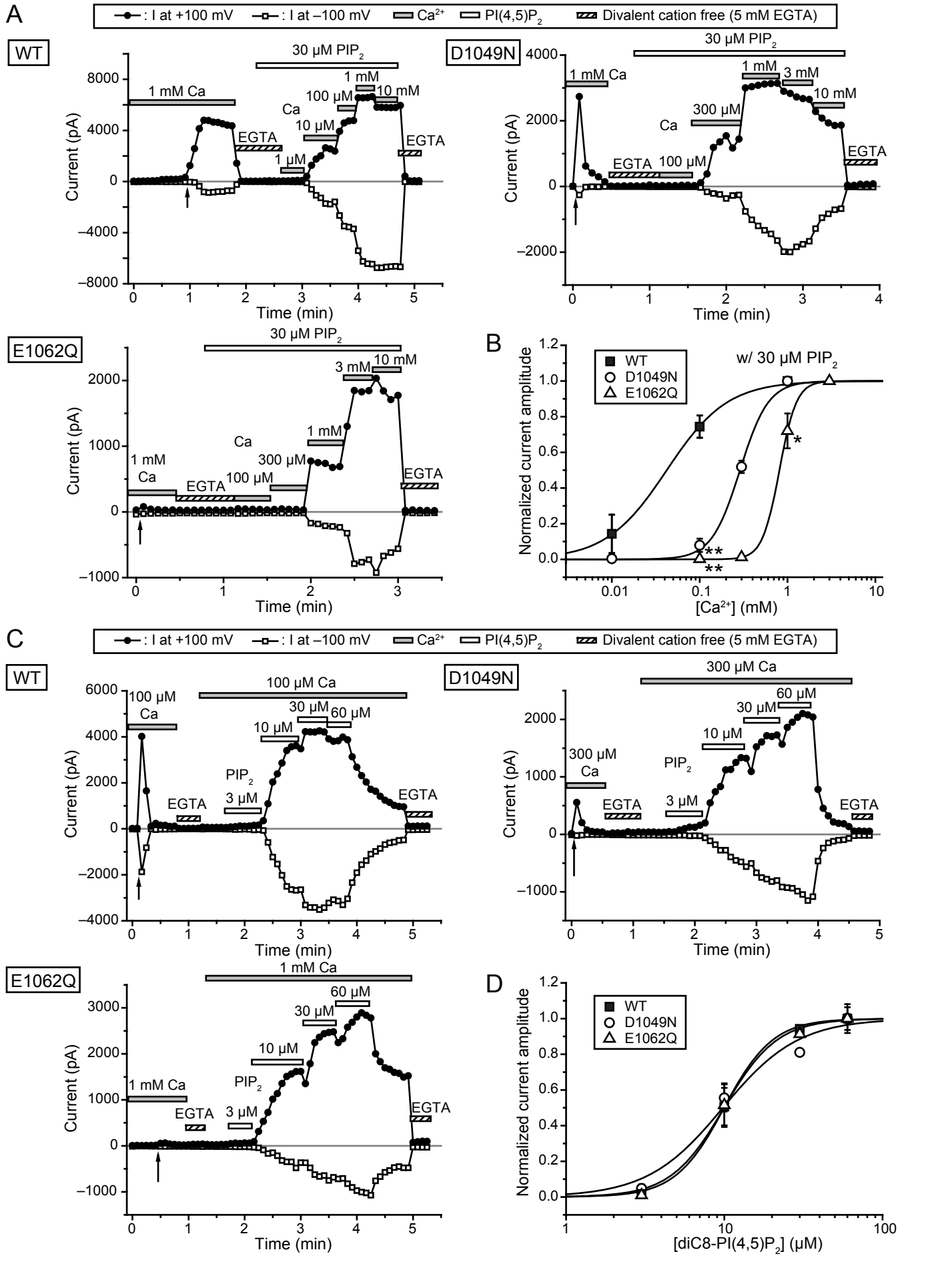

Figure 9, Yamaguchi, *et al.*

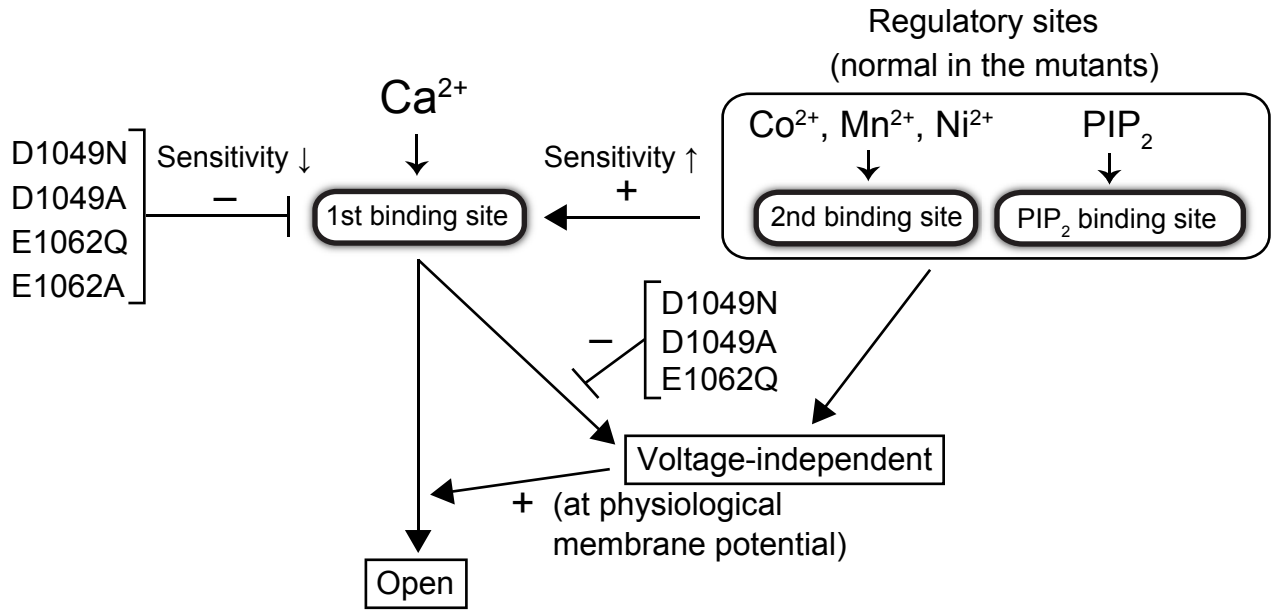

Figure 10, Yamaguchi, *et al.*